Research Paper
Computational Methods for Differential Equations
http://cmde.tabrizu.ac.ir
Vol. *, No. *, *, pp. 1-27
DOI:10.22034/cmde.2024.61425.2643

Bioconvective Flow Surrounding a Thin Surgical Needle in Blood Incorporating Ternary Hybrid Nanoparticles

Ahmed S. Rashed [1,2,*], **Ehsan H. Nasr** [3], **and Samah M. Mabrouk** [1]

[1]Department of Physics and Engineering Mathematics, Faculty of Engineering, Zagazig university, Egypt.

[2]Basic Science Department, Faculty of Engineering, Delta University for Science and Technology, Gamasa, 11152, Egypt.

[3]Delta Higher Institute for Engineering and Technology, Mansoura, Egypt.

Abstract

Biological systems use fluid dynamics to coordinate group movements and spatial arrangement, which affect both their own dispersion and the dynamics of their surroundings. This behavior has been documented in a number of biological systems, such as bacterial colonies, algal blooms, and microbial suspensions. The current study examines the flow of a nanofluid via a vertical thin needle used in medical surgery. The nanofluid is composed of three types of nanoparticles: Fe3O4, copper oxide (CuO), and copper (Cu) that are dispersed in a base fluid of blood. Additionally, the nanofluid contains gyrotactic bacteria. Furthermore, in the presence of a magnetic field, the incompressible liquid conducts current. The nanofluid model considers both Brownian motion and thermophoresis. The Runge-Kutta and shooting approach is used to numerically solve transformed ODEs resulting from group method. The present study looked at the effects of several factors, including Prandtl number, Brownian motion coefficient, Thermophoresis diffusion coefficient, Microorganism diffusion coefficient, concentration difference, temperature difference, Schmidt number, bioconvection Peclet number, Lewis number, and magnetic diffusivity. The findings indicate that velocity decreases with rising Pr, Lb and Sc and increases with D_B, D_T, D_n, δc, δt, and Pe. In contrast, temperature decreases with increasing Pr, D_B, and δc and increases with rising δt. Bacterial density, on the other hand, decreases with rising Pr and D_B and increases with D_T, D_n, and Sc. whereas the magnetic field grows as η_0 increases. We will also use graphs to illustrate the physical significance of the current parameters.

Keywords. Bioconvection, Hybrid nanofluid, Thermophoresis diffusion coefficient.

2010 Mathematics Subject Classification. 65L05, 34K06, 34K28.

1. Introduction

The phenomenon of fluid motion or convection known as "bioconvection" is brought about by the combined activity of microorganisms such as bacteria or algae inside a fluid medium. The synchronized migration of microorganisms causes the fluid to take on patterns, currents, or flow structures. Microorganisms in bioconvection exhibit directed motion due to their own movement, which is frequently accomplished by using cilia or flagella. As they move, these microorganisms push or pull on the fluid around them to create fluid flow. Large-scale flow patterns are formed as a result of the interaction between microorganisms and fluid.

Nanofluids are colloidal suspensions of nanoparticles scattered throughout a base fluid. These fluids have better qualities than the basic fluid alone, making them appropriate for a variety of uses. Nanofluids remain an important area of study, with continuous studies aimed at improving their characteristics, discovering novel nanoparticle materials, and broadening their uses across industries. Physical Characteristics of Specific Nanoparticles:

1. Magnetite (Fe_3O_4):

Because Fe_3O_4 is superparamagnetic, it may be controlled by applying external magnetic fields. This feature is

Received: 29 April 2024 ; Accepted: 25 November 2024.
∗ Corresponding author. Email: ahmed.s.rashed@gmail.com .

especially helpful in medical settings where localized heating can improve therapeutic efficacy, such as focused medication administration and the treatment of hyperthermia. Fe3O4 is also appropriate for in vivo research due to its biocompatibility, which lowers the possibility of negative bloodstream responses.

2. Copper Oxide (CuO):
Excellent heat conductivity and antimicrobial qualities are well-known attributes of copper oxide. Its absorption into blood may improve tissue temperature control, which is important for doing surgery or treating localized infections. Moreover, CuO's antibacterial properties can aid in lowering the risk of infections related to implants and medical equipment.

3. Copper (Cu):
One characteristic that sets copper nanoparticles apart is their unique electrical and thermal conductivity. Cu nanoparticles can enhance heat transmission characteristics when dissolved in blood, which may be advantageous for treating hyperthermia. Furthermore, copper has the ability to improve cellular respiration and oxygen transport, which is advantageous for medicinal applications, especially for disorders needing increased metabolic activity.

4. Blood Dynamics-Related Relevance:
Red blood cells, white blood cells, platelets, and plasma make up the complex biological fluid known as blood. Maintaining appropriate circulation and oxygen supply depends on its rheological characteristics. These characteristics change when Fe_3O_4, CuO, and Cu nanoparticles are added, which may result in better flow characteristics and better heat management.

Ongoing research is helping to better understan the bioconvection and its significance in biological and ecological systems. S. Siddiqa et al. [53] examined Numerical solutions of gyrotactic microorganism-induced nanofluid bioconvection along a vertically wavy cone. B. Shen et al. [52] studied temperature fluctuations and velocity slip during the bioconvection thermal transfer of a nanofluid across a stretched sheet. S. A. A. Shah et al. [51] investigated the impact of bioconvection on the motion of Prandtl hybrid nanofluid across a sheet of stretched fabric using chemical reaction and a motile microbe. S. Saleem et al. [49] examined the phenomena of magnetic Jeffrey nanofluid bioconvection over a revolving vertical cone caused by gyrotactic microorganisms. A. Rashad and H. A. Nabwey [42] examined the gyrotactic combined bioconvection movement of a nanofluid while investigating the convective boundary condition of a circular cylinder. M. V. S. Rao et al. [41] examined how gyrotactic microorganisms in a convectional nanofluid flow around an isothermal vertically cone embedded within a surface that is porous holding chemically reactive substances might cause bioconvection. C. S. Raju and N. Sandeep [40] studied two distinct methods for handling unstable mass and heat transfer in a bioconvection flow that is going to approach a rotating cone or plate in a rotating fluid. C. Raju and N. Sandeep [39] examined the mass and heat transfer through a spinning disk or cone with cross diffusion in a non-Newtonian magnetohydrodynamic (MHD) bio-convection flow. V. Puneeth et al. [38] examined the effect of bioconvection on a pseudoplastic nanofluid's free stream flow past a rotating cone. P. Patil et al. [37] investigated the effects on bioconvective periodical MHD Eyring-Powell flow of fluid around a rotary cone of various diffusions and oxytactic microorganisms. D. Pal and S. K. Mondal [36] examined MHD nanofluid bioconvection between gyrotactic microorganisms and heat radiation across an exponentially stretching sheet. W. N. Mutuku and O. D. Makinde [35] explored the phenomena of gyrotactic microorganism-induced hydromagnetic bioconvection of the nanofluid over a porous vertical plate. A. V. Kuznetsov [29] used oxytactic microorganisms to study the phenomena of nanofluid bioconvection in media that is porous. A. V. Kuznetsov [30] examined oscillatory instability in water-based solutions including nanoparticles and oxytactic microorganisms during nanofluid bioconvection. A. Kuznetsov [28] looked at the interaction of microorganisms, oxytactic up-swimming, dispersion of nanoparticles, and subsurface heating/cooling are all involved in nanofluid bioconvection. W. A. Khan et al. [27] examined the gyrotactic microorganism-containing truncated cone's spontaneous bioconvection flow across a nanofluid. W. Khan and O. Makinde et al. [26] investigated how MHD nanofluid bioconvection across a stretched sheet heated by convection is affected by gyrotactic microorganisms. P. P. Humane et al. [25] examined the impact of bioconvection on the movement of a chemically reactive nanofluid made by Casson flowing through an inclined. N. Begum et al. [13] investigated changing thermophysical characteristics of nanofluid bioconvection. C. S. Balla et al. [12] examined bioconvection in an oxytactic microbial culture in a porosity square cavity saturated with nanofluid. A. U. Awan et al. [11] employed an exponential source of heat and motile microorganisms, the impacts of bioconvection were examined on Williamson nanofluid flows on a

stretched sheet. M. I. Asjad et al. [10] examined the effects of chemical reactions and bioconvection on the flow of MHD nanofluids because of exponential stretching sheet. O. Anwar Bég [9] examined models and computation for nonlinear multiphysical laminar nanofluid bioconvection flows. N. A. Amirsom et al. [8] looked over Multidimensional bioconvection flow of nanofluid from a bi-axial sheet of stretching caused by isotropic slip. R. Alluguvelli et al. [6] investigated the bioconvection of nanofluids in porous enclosures with viscous dissipation. B. Ali et al. [5] examined the Cattaneo-Christov and bioconvection effects in micropolar dependent nanofluid flow simulation using finite elements over a vertically extended sheet. K. A. M. Alharbi et al. [3] examined the numerical solution for the Maxwell-Sutterby nanofluid flow in a sheet that was stretched with thermal energy. S. A. Alavi et al. [2] examined an algorithmic approach to fractional optimum control issues with the Mott polynomial operational matrix. A. R. Haghighi and N. Aliashrafi [18] analyzed pulsatile blood flow via a stenosed artery under the influence of a magnetic field, mathematically modeled. A. R. Haghighi and R. Pralhad [20] studied blood flow mathematical modeling under the influence of body forces and magnetism on the human body. A. R. Haghighi and N. Aliashrafi [19] examined and analyzed mathematical simulations of pulsatile blood flow and heat transmission in a vibrating and magnetic environment. A. R. Haghighi et al.[21] evaluated a tacit method for the micropolar fluid model of blood flow in response to bodily acceleration. Additional studies on bioconvection have been conducted [4, 7, 14–17, 22–24]. This study investigates the flow of a nanofluid through a vertical thin needle used in medical surgery. The nanofluid is made up of three types of nanoparticles $Fe_3O_4, CuO, and Cu$, which are scattered in a base fluid of blood. Furthermore, the nanofluid contains gyrotactic microorganisms. Furthermore, in the presence of a magnetic field, the incompressible liquid conducts electricity. The nanofluid model takes into account both Brownian motion and Thermophoresis. The current study examined the impacts of many elements including Prandtl number, Pr, Brownian motion coefficient, D_B, Thermophoresis diffusion coefficient, D_T, microorganism diffusion coefficient, D_n, concentration difference ratio, δC,temperature difference, Δt , Schmidt number, Sc, bioconvection Peclet number, Pe , Lewis number, Lb , and magnetic diffusivity, η_0.

2. Mathematical Formulation

Bioconvection is the collective motion of microorganisms, which occurs in response to environmental gradients such as light, temperature, or concentration differences. The cone model is a mathematical framework that describes bioconvection in suspensions of swimming microorganisms. The goal of this study is to investigate the steady flow of a viscous, incompressible nanofluid along a thin, vertical needle containing gyrotactic bacteria and three distinct nanoparticles. The magnetic field characteristics imparted to the nanoparticles cause their electrical conductivity. The radius of the needle is $r = R(x)$. Figure 1 shows that the axial component is x, and the radially oriented component is r. The electric conductivity and density of the hybrid nanofluid are denoted by the symbols σ_{hnf} and ρ_{hnf}, respectively, while the cone temperature is represented by T_w. The symbols u and v indicate the velocity of the fluid components. The concentration continuity equation calculates a volumetric proportion of nanoparticle concentration, c. To complete the mathematical framework of the current work, a microbe continuity equation is provided. For the mathematical model, Equations (2.1)-(2.7) define it, whereas Figure 1 depicts the precise model.

$$ru_x + rv_r + v = 0, \tag{2.1}$$

$$\begin{aligned} u_t + uu_x + vu_r &= \frac{\mu_{hnf}}{r\rho_{hnf}}\frac{\partial}{\partial r}(ru_r) - \frac{\sigma B_0^2 u}{\rho_{hnf}} + \beta g(T - T_\infty) - \frac{\rho_p - \rho_f}{\rho_{hnf}} g(C - C_\infty) \\ &- \frac{\rho_m - \rho_f}{\rho_{hnf}} g(N - N_\infty) + \frac{\mu_e H_2}{4\pi\rho_{hnf}}(H_{1x} + H_{1r}), \end{aligned} \tag{2.2}$$

$$\begin{aligned} T_t + uT_x + vT_r &= \frac{\alpha_{hnf}}{r}\frac{\partial}{\partial r}(rT_r) + \frac{\alpha_{hnf}}{K_{hnf}}\mu_{hnf}(u_r)^2 + \frac{\alpha_{hnf}\sigma B_0^2 u^2}{k_{hnf}} - \frac{1}{(\rho c_p)_{hnf}}\frac{1}{r}\left(\frac{16\sigma^* T_\infty^3}{3k^*}\right)\frac{\partial}{\partial r}(rT_r) \\ &+ \tau\left[\frac{D_T}{T_\infty}{T_r}^2 + \frac{D_B}{\Delta C}T_r C_r\right] + \frac{Q_0}{(\rho c_p)_{hnf}}(T - T_\infty), \end{aligned} \tag{2.3}$$

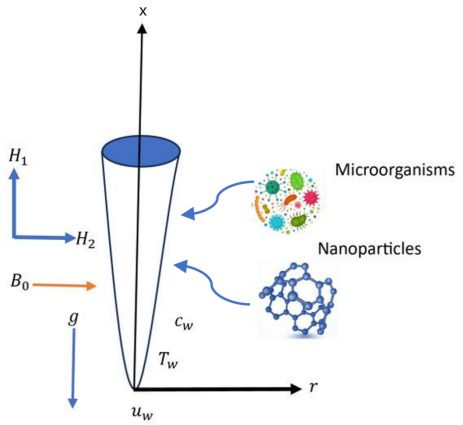

FIGURE 1. Physical illustration of the problem.

$$C_t + uC_x + vC_r = D_B C_{rr} + \frac{\Delta C D_T}{T_\infty} T_{rr}, \tag{2.4}$$

$$N_t + uN_x + vN_r + \frac{bw_c}{C_w - C_\infty}\left[\frac{\partial}{\partial r} NC_r\right] = D_n N_{rr}, \tag{2.5}$$

$$H_{1t} + uH_{1x} + vH_{1r} = \frac{\eta_0}{r}\left(\frac{\partial}{\partial r}(rH_{1r})\right), \tag{2.6}$$

$$H_{2t} + uH_{2x} + vH_{2r} = \frac{\eta_0}{r}\left(\frac{\partial}{\partial r}(rH_{2r})\right). \tag{2.7}$$

Subjected to:

$$\begin{aligned} &At \quad r = R(x) = \left(\frac{\nu_{hnf}}{u_w + u_\infty} r_0 x\right)^{\frac{1}{2}} \\ &u = u_w,\ v = 0,\ H_1 = H_{1w},\ H_2 = H_{2w},\ T = T_w,\ \ C = C_w,\ \ N = N_w \\ &At \quad r \to \infty \\ &u = 0,\ H_1 = 0,\ H_2 = 0,\ T = T_\infty,\ \ C = C_\infty,\ \ N = N_\infty \end{aligned} \tag{2.8}$$

Normalization process:

$$\begin{aligned} &u(x,r,t) = u^*(x,r,t)\ u_w(x,t), \\ &v(x,r,t) = v^*(x,r,t)\ v_w(x,t), \\ &H_1(x,r,t) = {H_1}^*(x,r,t)\ H_{1w}(x,t), \\ &H_2(x,r,t) = {H_2}^*(x,r,t)\ H_{2w}(x,t), \\ &T = \Delta T\theta + T_\infty, \\ &C = \Delta C C^* + c_\infty, \\ &N = \Delta N N^* + N_\infty. \end{aligned} \tag{2.9}$$

Equations (2.1)-(2.7) can be transformed to:

$$ru^*\frac{\partial u_w}{\partial x} + ru_w\frac{\partial u^*}{\partial x} + rv_w\frac{\partial v^*}{\partial r} + v^* v_w = 0, \tag{2.10}$$

$$u^*\frac{\partial u_w}{\partial t}+u_w\frac{\partial u^*}{\partial t}\ +u^*u_wu^*\frac{\partial u_w}{\partial x}+u^*u_wu_w\frac{\partial u^*}{\partial x}+v^*v_wu_w\frac{\partial u^*}{\partial r}-\frac{\mu_{hnf}}{r\rho_{hnf}}u_wr\ \frac{\partial^2u^*}{\partial r^2}-\frac{\mu_{hnf}}{r\rho_{hnf}}u_w\frac{\partial u^*}{\partial r}$$
$$+\frac{\sigma B_0^2u^*u_w}{\rho_{hnf}}-\beta g(\Delta T\theta)+\frac{\rho_p-\rho_f}{\rho_{hnf}}g\left(\Delta CC^*\right)+\frac{\rho_m-\rho_f}{\rho_{hnf}}g\left(\Delta NN^*\right)-\frac{\mu_e{H_2}^*H_{2w}}{4\pi\rho_{hnf}}{H_1}^*\frac{\partial H_{1w}}{\partial x}$$
$$-\frac{\mu_e{H_2}^*H_{2w}}{4\pi\rho_{hnf}}H_{1w}\frac{\partial {H_1}^*}{\partial x}-\frac{\mu_e{H_2}^*H_{2w}}{4\pi\rho_{hnf}}H_{1w}\frac{\partial {H_1}^*}{\partial r}=0, \tag{2.11}$$
$$\frac{\partial\theta}{\partial t}+u^*u_w\frac{\partial\theta}{\partial x}+v^*v_w\frac{\partial\theta}{\partial r}-\alpha_{hnf}\frac{\partial^2\theta}{\partial r^2}-\frac{\alpha_{hnf}}{r}\frac{\partial\theta}{\partial r}-\frac{\alpha_{hnf}}{\Delta TK_{hnf}}\mu_{hnf}\left(u_w\frac{\partial u^*}{\partial r}\right)^2$$
$$-\frac{\alpha_{hnf}\sigma B_0^2\left(u^*u_w\right)^2}{\Delta Tk_{hnf}}+\frac{1}{\left(\rho c_p\right)_{hnf}}\left(\frac{16\sigma^*T_\infty^3}{3k^*}\right)\frac{\partial^2\theta}{\partial r^2}+\frac{1}{\left(\rho c_p\right)_{hnf}}\frac{1}{r}\left(\frac{16\sigma^*T_\infty^3}{3k^*}\right)\frac{\partial\theta}{\partial r}$$
$$-\tau\frac{D_T}{T_\infty}\Delta T\left(\frac{\partial\theta}{\partial r}\right)^2-\tau\frac{D_B}{\Delta C}\frac{\partial\theta}{\partial r}\Delta C\frac{\partial C^*}{\partial r}-\frac{Q_0}{\left(\rho c_p\right)_{hnf}}\theta=0, \tag{2.12}$$

$$\Delta C\frac{\partial C^*}{\partial t}+u^*u_w\Delta C\frac{\partial C^*}{\partial x}+v^*v_w\Delta C\frac{\partial C^*}{\partial r}=D_B\Delta C\frac{\partial^2C^*}{\partial r^2}+\frac{\Delta CD_T}{T_\infty}\Delta T\frac{\partial^2\theta}{\partial r^2}, \tag{2.13}$$
$$\frac{\partial N^*}{\partial t}+u^*u_w\frac{\partial N^*}{\partial x}+v^*v_w\frac{\partial N^*}{\partial r}+bw_cN^*\frac{\partial^2C^*}{\partial r^2}+bw_c\frac{N_\infty}{\Delta N}\frac{\partial^2C^*}{\partial r^2}+bw_c\frac{\partial C^*}{\partial r}\frac{\partial N^*}{\partial r}-D_n\frac{\partial^2N^*}{\partial r^2}=0, \tag{2.14}$$
$${H_1}^*\frac{\partial H_{1w}}{\partial t}+H_{1w}\frac{\partial {H_1}^*}{\partial t}+u^*u_w{H_1}^*\frac{\partial H_{1w}}{\partial x}+u^*u_wH_{1w}\frac{\partial {H_1}^*}{\partial x}+v^*v_wH_{1w}\frac{\partial {H_1}^*}{\partial r}$$
$$-\eta_0H_{1w}\ \frac{\partial^2{H_1}^*}{\partial r^2}-\frac{\eta_0}{r}H_{1w}\frac{\partial {H_1}^*}{\partial r}=0, \tag{2.15}$$
$${H_2}^*\frac{\partial H_{2w}}{\partial t}+H_{2w}\frac{\partial {H_2}^*}{\partial t}+u^*u_w{H_2}^*\frac{\partial H_{2w}}{\partial x}+u^*u_wH_{2w}\frac{\partial {H_2}^*}{\partial x}+v^*v_wH_{2w}\frac{\partial {H_2}^*}{\partial r}$$
$$-\eta_0H_{2w}\ \frac{\partial^2{H_2}^*}{\partial r^2}-\frac{\eta_0}{r}H_{2w}\frac{\partial {H_2}^*}{\partial r}=0. \tag{2.16}$$

$$At\quad r=R(x)=\left(\frac{\nu_{hnf}}{u_w+u_\infty}r_0x\right)^{\frac{1}{2}},$$
$$u^*=1,v^*=0,{H_1}^*=1,{H_2}^*=1,\theta=1,C^*=1,N^*=1, \tag{2.17}$$
$$At\quad r\to\infty,$$
$$u^*=0,{H_1}^*=0,{H_2}^*=0,\theta=0,C^*=0,N^*=0.$$

3. Modification of system invariant group

A two-parameter group topology $(\alpha_1,\ \alpha_2)$ is used to transform the mathematical model into a system of similar ODEs based on the similarity variable, η.

3.1. **Similarity Transformation.**

Let's take the group structure in the form:

$$G:\overline{S}=K^s\left(\alpha_1,\alpha_2\right)S+Q^s(\alpha_1,\alpha_2). \tag{3.1}$$

The system variables are represented by the letter S, and the differential coefficient functions are represented by the actual values of K^s and Q^s. The typical way to represent partial derivatives is as follows:

$$\left.\begin{array}{l}\overline{S}_{\overline{i}}=\left(\frac{K^s}{K^i}\right)S_i,\\ \overline{S}_{\overline{ij}}=\left(\frac{K^s}{K^iK^j}\right)S_{ij},\end{array}\right\}\ i=r,x,t,\ and\ j=r,x,t. \tag{3.2}$$

3.2. **The Analysis of the problem.**
Equation (2.10), using the previous relations (3.1) and (3.2), becomes:

$$\overline{ru^*}\frac{\partial\overline{u_w}}{\partial\overline{x}}+\overline{ru_w}\frac{\partial\overline{u^*}}{\partial\overline{x}}+\overline{rv_w}\frac{\partial\overline{v^*}}{\partial\overline{r}}+\overline{v^*v_w}=H_1\left(\alpha_1,\alpha_2\right)\left[ru^*\frac{\partial u_w}{\partial x}+ru_w\frac{\partial u^*}{\partial x}+rv_w\frac{\partial v^*}{\partial r}+v^*v_w\right], \tag{3.3}$$

$H_1\left(\alpha_1,\alpha_2\right)$ is the equivalency parameter, and the slashes denote the adjusted variables. By combining (3.1) and (3.2) into (3.3), the following results can be obtained:

$$\begin{aligned}&\frac{k^rk^{u^*}k^{u_w}}{k^x}ru^*\frac{\partial u_w}{\partial x}+\frac{k^rk^{u^*}k^{u_w}}{k^x}ru_w\frac{\partial u^*}{\partial x}+\frac{k^rk^{v^*}k^{v_w}}{k^r}rv_w\frac{\partial v^*}{\partial r}+k^{v^*}k^{v_w}v^*v_w\\&=H_1\left(\alpha_1,\alpha_2\right)\left[ru^*\frac{\partial u_w}{\partial x}+ru_w\frac{\partial u^*}{\partial x}+rv_w\frac{\partial v^*}{\partial r}+v^*v_w\right].\end{aligned} \tag{3.4}$$

Similarly, Equations (2.11)-(2.16) become:

$$\begin{aligned}&\frac{k^{u^*}k^{u_w}}{k^t}u^*\frac{\partial u_w}{\partial t}+\frac{k^{u^*}k^{u_w}}{k^t}u_w\frac{\partial u^*}{\partial t}+\frac{k^{u^*}k^{u_w}k^{u^*}k^{u_w}}{k^x}u^*u_wu^*\frac{\partial u_w}{\partial x}+\frac{k^{u^*}k^{u_w}k^{u^*}k^{u_w}}{k^x}u^*u_wu_w\frac{\partial u^*}{\partial x}\\&+\frac{k^{v^*}k^{v_w}k^{u^*}k^{u_w}}{k^r}v^*v_wu_w\frac{\partial u^*}{\partial r}-\frac{\mu_{hnf}}{r\rho_{hnf}}\frac{k^rk^{u^*}k^{u_w}}{\left(k^r\right)^2}u_wr\frac{\partial^2u^*}{\partial r^2}-\frac{\mu_{hnf}}{r\rho_{hnf}}\frac{k^{u^*}k^{u_w}}{k^r}u_w\frac{\partial u^*}{\partial r}\\&+k^{u^*}k^{u_w}\frac{\sigma B_0^2u^*u_w}{\rho_{hnf}}-k^\theta\beta g(\Delta T\theta)+\frac{\rho_p-\rho_f}{\rho_{hnf}}k^{C^*}g\left(\Delta CC^*\right)+\frac{\rho_m-\rho_f}{\rho_{hnf}}k^{N^*}g\left(\Delta NN^*\right)\\&-\frac{k^{H_2{}^*}k^{H_{2w}}k^{H_1{}^*}k^{H_{1w}}}{k^x}\frac{\mu_e{H_2}^*H_{2w}}{4\pi\rho_{hnf}}{H_1}^*\frac{\partial H_{1w}}{\partial x}-\frac{k^{H_2{}^*}k^{H_{2w}}k^{H_1{}^*}k^{H_{1w}}}{k^x}\frac{\mu_e{H_2}^*H_{2w}}{4\pi\rho_{hnf}}H_{1w}\frac{\partial{H_1}^*}{\partial x}\\&-\frac{k^{H_2{}^*}k^{H_{2w}}k^{H_1{}^*}k^{H_{1w}}}{k^r}\frac{\mu_e{H_2}^*H_{2w}}{4\pi\rho_{hnf}}H_{1w}\frac{\partial{H_1}^*}{\partial r}=H_2\left(\alpha_1,\alpha_2\right)\\&\left[u^*\frac{\partial u_w}{\partial t}+u_w\frac{\partial u^*}{\partial t}+u^*u_wu^*\frac{\partial u_w}{\partial x}+u^*u_wu_w\frac{\partial u^*}{\partial x}+v^*v_wu_w\frac{\partial u^*}{\partial r}\right.\\&-\frac{\mu_{hnf}}{r\rho_{hnf}}u_wr\frac{\partial^2u^*}{\partial r^2}-\frac{\mu_{hnf}}{r\rho_{hnf}}u_w\frac{\partial u^*}{\partial r}+\frac{\sigma B_0^2u^*u_w}{\rho_{hnf}}-\beta g(\Delta T\theta)+\frac{\rho_p-\rho_f}{\rho_{hnf}}g\left(\Delta CC^*\right)\\&+\frac{\rho_m-\rho_f}{\rho_{hnf}}g\left(\Delta NN^*\right)-\frac{\mu_e{H_2}^*H_{2w}}{4\pi\rho_{hnf}}{H_1}^*\frac{\partial H_{1w}}{\partial x}-\frac{\mu_e{H_2}^*H_{2w}}{4\pi\rho_{hnf}}H_{1w}\frac{\partial{H_1}^*}{\partial x}-\\&\left.\frac{\mu_e{H_2}^*H_{2w}}{4\pi\rho_{hnf}}H_{1w}\frac{\partial{H_1}^*}{\partial r}\right],\end{aligned} \tag{3.5}$$

$$\frac{k^{\theta}}{k^{t}}\frac{\partial\theta}{\partial t}+\frac{k^{u^{*}}k^{u_{w}}k^{\theta}}{k^{x}}u^{*}u_{w}\frac{\partial\theta}{\partial x}+\frac{k^{v^{*}}k^{v_{w}}k^{\theta}}{k^{r}}v^{*}v_{w}\frac{\partial\theta}{\partial r}-\alpha_{hnf}\frac{k^{\theta}}{\left(k^{r}\right)^{2}}\frac{\partial^{2}\theta}{\partial r^{2}}-\frac{\alpha_{hnf}}{r}\frac{k^{\theta}}{k^{r}}\frac{\partial\theta}{\partial r}$$
$$-\frac{\alpha_{hnf}}{\Delta TK_{hnf}}\mu_{hnf}\left(\frac{k^{u^{*}}k^{u_{w}}}{k^{r}}u_{w}\frac{\partial u^{*}}{\partial r}\right)^{2}-\frac{\alpha_{hnf}\sigma B_{0}^{2}\left(k^{u^{*}}k^{u_{w}}u^{*}u_{w}\right)^{2}}{\Delta Tk_{hnf}}$$
$$+\frac{1}{\left(\rho c_{p}\right)_{hnf}}\left(\frac{16\sigma^{*}T_{\infty}^{3}}{3k^{*}}\right)\frac{k^{\theta}}{\left(k^{r}\right)^{2}}\frac{\partial^{2}\theta}{\partial r^{2}}+\frac{1}{\left(\rho c_{p}\right)_{hnf}}\frac{1}{r}\frac{k^{\theta}}{\left(k^{r}\right)^{2}}\left(\frac{16\sigma^{*}T_{\infty}^{3}}{3k^{*}}\right)\frac{\partial\theta}{\partial r}-\tau\frac{D_{T}}{T_{\infty}}\Delta T\left(\frac{k^{\theta}}{k^{r}}\frac{\partial\theta}{\partial r}\right)^{2}$$
$$-\tau\frac{D_{B}}{\Delta C}\frac{k^{\theta}}{k^{r}}\frac{\partial\theta}{\partial r}\Delta C\frac{k^{C^{*}}}{k^{r}}\frac{\partial C^{*}}{\partial r}-\frac{Q_{0}}{\left(\rho c_{p}\right)_{hnf}}k^{\theta}\theta=H_{3}\left(\alpha_{1},\alpha_{2}\right)\left[\frac{\partial\theta}{\partial t}+u^{*}u_{w}\frac{\partial\theta}{\partial x}+v^{*}v_{w}\frac{\partial\theta}{\partial r}-\alpha_{hnf}\frac{\partial^{2}\theta}{\partial r^{2}}\right.$$
$$-\frac{\alpha_{hnf}}{r}\frac{\partial\theta}{\partial r}-\frac{\alpha_{hnf}}{\Delta TK_{hnf}}\mu_{hnf}\left(u_{w}\frac{\partial u^{*}}{\partial r}\right)^{2}-\frac{\alpha_{hnf}\sigma B_{0}^{2}\left(u^{*}u_{w}\right)^{2}}{\Delta Tk_{hnf}}+\frac{1}{\left(\rho c_{p}\right)_{hnf}}\left(\frac{16\sigma^{*}T_{\infty}^{3}}{3k^{*}}\right)\frac{\partial^{2}\theta}{\partial r^{2}}$$
$$\left.+\frac{1}{\left(\rho c_{p}\right)_{hnf}}\frac{1}{r}\left(\frac{16\sigma^{*}T_{\infty}^{3}}{3k^{*}}\right)\frac{\partial\theta}{\partial r}-\tau\frac{D_{T}}{T_{\infty}}\Delta T\left(\frac{\partial\theta}{\partial r}\right)^{2}-\tau\frac{D_{B}}{\Delta C}\frac{\partial\theta}{\partial r}\Delta C\frac{\partial C^{*}}{\partial r}-\frac{Q_{0}}{\left(\rho c_{p}\right)_{hnf}}\theta\right], \tag{3.6}$$

$$\frac{k^{C^{*}}}{k^{t}}\frac{\partial C^{*}}{\partial t}+\frac{k^{u^{*}}k^{u_{w}}k^{C^{*}}}{k^{x}}u^{*}u_{w}\frac{\partial C^{*}}{\partial x}+\frac{k^{v^{*}}k^{v_{w}}k^{C^{*}}}{k^{r}}v^{*}v_{w}\frac{\partial C^{*}}{\partial r}-D_{B}\frac{k^{C^{*}}}{\left(k^{r}\right)^{2}}\frac{\partial^{2}C^{*}}{\partial r^{2}}-\frac{D_{T}}{T_{\infty}}\Delta T\frac{k^{\theta}}{\left(k^{r}\right)^{2}}\frac{\partial^{2}\theta}{\partial r^{2}}$$
$$=H_{4}\left(\alpha_{1},\alpha_{2}\right)\left[\frac{\partial C^{*}}{\partial t}+u^{*}u_{w}\frac{\partial C^{*}}{\partial x}+v^{*}v_{w}\frac{\partial C^{*}}{\partial r}-D_{B}\frac{\partial^{2}C^{*}}{\partial r^{2}}-\frac{D_{T}}{T_{\infty}}\Delta T\frac{\partial^{2}\theta}{\partial r^{2}}\right], \tag{3.7}$$

$$\frac{k^{N^{*}}}{k^{t}}\frac{\partial N^{*}}{\partial t}+\frac{k^{u^{*}}k^{u_{w}}k^{N^{*}}}{k^{x}}u^{*}u_{w}\frac{\partial N^{*}}{\partial x}+\frac{k^{v^{*}}k^{v_{w}}k^{N^{*}}}{k^{r}}v^{*}v_{w}\frac{\partial N^{*}}{\partial r}+bw_{c}\frac{k^{N^{*}}k^{C^{*}}}{\left(k^{r}\right)^{2}}N^{*}\frac{\partial^{2}C^{*}}{\partial r^{2}}$$
$$+bw_{c}\frac{N_{\infty}}{\Delta N}\frac{k^{C^{*}}}{\left(k^{r}\right)^{2}}\frac{\partial^{2}C^{*}}{\partial r^{2}}+bw_{c}\frac{k^{N^{*}}k^{C^{*}}}{\left(k^{r}\right)^{2}}\frac{\partial C^{*}}{\partial r}\frac{\partial N^{*}}{\partial r}-D_{n}\frac{k^{N^{*}}}{\left(k^{r}\right)^{2}}\frac{\partial^{2}N^{*}}{\partial r^{2}}=H_{5}\left(\alpha_{1},\alpha_{2}\right)\left[\frac{\partial N^{*}}{\partial t}+\right. \tag{3.8}$$
$$\left.u^{*}u_{w}\frac{\partial N^{*}}{\partial x}+v^{*}v_{w}\frac{\partial N^{*}}{\partial r}+bw_{c}N^{*}\frac{\partial^{2}C^{*}}{\partial r^{2}}+bw_{c}\frac{N_{\infty}}{\Delta N}\frac{\partial^{2}C^{*}}{\partial r^{2}}+bw_{c}\frac{\partial C^{*}}{\partial r}\frac{\partial N^{*}}{\partial r}-D_{n}\frac{\partial^{2}N^{*}}{\partial r^{2}}\right],$$

$$\frac{k^{H_{1}{}^{*}}k^{H_{1w}}}{k^{t}}H_{1}{}^{*}\frac{\partial H_{1w}}{\partial t}+\frac{k^{H_{1}{}^{*}}k^{H_{1w}}}{k^{t}}H_{1w}\frac{\partial H_{1}{}^{*}}{\partial t}+\frac{k^{u^{*}}k^{u_{w}}k^{H_{1}{}^{*}}k^{H_{1w}}}{k^{x}}u^{*}u_{w}H_{1}{}^{*}\frac{\partial H_{1w}}{\partial x}$$
$$+\frac{k^{u^{*}}k^{u_{w}}k^{H_{1}{}^{*}}k^{H_{1w}}}{k^{x}}u^{*}u_{w}H_{1w}\frac{\partial H_{1}{}^{*}}{\partial x}+\frac{k^{v^{*}}k^{v_{w}}k^{H_{1}{}^{*}}k^{H_{1w}}}{k^{r}}v^{*}v_{w}H_{1w}\frac{\partial H_{1}{}^{*}}{\partial r}$$
$$-\eta_{0}\frac{k^{H_{1}{}^{*}}k^{H_{1w}}k^{r}}{\left(k^{r}\right)^{2}}H_{1w}\frac{\partial^{2}H_{1}{}^{*}}{\partial r^{2}}-\frac{k^{H_{1}{}^{*}}k^{H_{1w}}}{\left(k^{r}\right)^{2}}\frac{\eta_{0}}{r}H_{1w}\frac{\partial H_{1}{}^{*}}{\partial r}=H_{6}\left(\alpha_{1},\alpha_{2}\right)\left[H_{1}{}^{*}\frac{\partial H_{1w}}{\partial t}\right. \tag{3.9}$$
$$+H_{1w}\frac{\partial H_{1}{}^{*}}{\partial t}+u^{*}u_{w}H_{1}{}^{*}\frac{\partial H_{1w}}{\partial x}+u^{*}u_{w}H_{1w}\frac{\partial H_{1}{}^{*}}{\partial x}+v^{*}v_{w}H_{1w}\frac{\partial H_{1}{}^{*}}{\partial r}$$
$$\left.-\eta_{0}H_{1w}\frac{\partial^{2}H_{1}{}^{*}}{\partial r^{2}}-\frac{\eta_{0}}{r}H_{1w}\frac{\partial H_{1}{}^{*}}{\partial r}\right],$$

$$\frac{k^{H_2{}^*}k^{H_{2w}}}{k^t}H_2{}^*\frac{\partial H_{2w}}{\partial t}+\frac{k^{H_2{}^*}k^{H_{2w}}}{k^t}H_{2w}\frac{\partial H_2{}^*}{\partial t}+\frac{k^{u^*}k^{u_w}k^{H_2{}^*}k^{H_{2w}}}{k^x}u^*u_wH_2{}^*\frac{\partial H_{2w}}{\partial x}$$
$$+\frac{k^{u^*}k^{u_w}k^{H_2{}^*}k^{H_{2w}}}{k^x}u^*u_wH_{2w}\frac{\partial H_2{}^*}{\partial x}+\frac{k^{v^*}k^{v_w}k^{H_2{}^*}k^{H_{2w}}}{k^r}v^*v_wH_{2w}\frac{\partial H_2{}^*}{\partial r}-\eta_0\frac{k^{H_2{}^*}k^{H_{2w}}k^r}{(k^r)^2}H_{2w}\frac{\partial^2 H_2{}^*}{\partial r^2}$$
$$-\frac{\eta_0}{r}\frac{k^{H_2{}^*}k^{H_{2w}}}{(k^r)^2}H_{2w}\frac{\partial H_2{}^*}{\partial r}=H_7(\alpha_1,\alpha_2)\left[H_2{}^*\frac{\partial H_{2w}}{\partial t}+H_{2w}\frac{\partial H_2{}^*}{\partial t}+u^*u_wH_2{}^*\frac{\partial H_{2w}}{\partial x}+u^*u_wH_{2w}\frac{\partial H_2{}^*}{\partial x}\right. \tag{3.10}$$
$$\left.+v^*v_wH_{2w}\frac{\partial H_2{}^*}{\partial r}-\eta_0H_{2w}\frac{\partial^2 H_2{}^*}{\partial r^2}-\frac{\eta_0}{r}H_{2w}\frac{\partial H_2{}^*}{\partial r}\right].$$

The following outcomes arise from the invariance condition:

$$K^{u_w}K^{u^*}{=}K^x=K^{v^*}K^{v_w}{=}K^r=K^t=K^{N^*}=K^{C^*}=K^\theta=K^{H_{2w}}K^{H_2^*}{=}K^{H_{1w}}K^{H_1^*}=\mathbf{1},$$
$$Q^{u_w}=Q^{u^*}=Q^{v_w}=Q^{v^*}=Q^{C^*}=Q^\theta=Q^{H_2^*}=Q^{H_1^*}=Q^{H_{1w}}=Q^{H_{2w}}=Q^{N^*}=0. \tag{3.11}$$

Finally, the structure of the group, G, becomes:

$$G:\begin{cases}G_1\begin{cases}\overline{x}=x+Q^x,\\ \overline{r}=r+Q^y,\\ \overline{t}=t+Q^t,\\ \cdot\end{cases}\\ G_2\begin{cases}\overline{C^*}=C^*,\\ \overline{\theta}=\theta,\\ \cdot\\ \overline{N^*}=N^*,\\ \overline{u}_w=K^{u_w}u_w,\\ \overline{v}_w=K^{v_w}v_w,\\ \cdot\\ \overline{H_{1w}}=K^{H_{1w}}H_{1w},\\ \overline{H_{2w}}=K^{H_{2w}}H_{2w},\\ \overline{u^*}=k^{u^*}u^*,\\ \overline{v^*}=k^{v^*}v^*,\\ \overline{H_1{}^*}=K^{H_1{}^*}H_1{}^*,\\ \overline{H_2{}^*}=K^{H_2{}^*}H_2{}^*.\end{cases}\end{cases} \tag{3.12}$$

3.3. **The complete conversion of the system's variables.**

The relation shown below, which is motivated by Morgan's theorem [34], is used to alter the system variables:

$$\sum_{i=1}^{14}(\gamma_iS_i+\delta_i)\frac{\partial q_i}{\partial S_i}=0. \tag{3.13}$$

The methodology minimizes the number of independent variables by employing a single similarity variable. The system's original variables are denoted by the symbol S_i, while the dependent variables u^*, u_e, u_w, v^*, v_e, v_w, w, c^*, θ, N^*, $H_1{}^*$, H_{1e}, $H_2{}^*$, H_{2e} become new, invariant variables. At this point, the coefficients γ_i *and* δ_i, are defined as

follows:

$$\begin{cases} \gamma_i = \frac{\partial K^{S_i}(\alpha)}{\partial \alpha}, \\ \delta_i = \frac{\partial Q^{S_i}(\alpha)}{\partial \alpha}. \end{cases} \tag{3.14}$$

3.4. **The modification of independent variables.**

Equation (3.13) has been used to combine the independent variables ($r,\ x,\ and\ t$) into a single similarity variable. By using the same procedures as described in references [31–33, 43–48, 50], the variables are provided by:

$$\eta = \pi(x,t)r. \tag{3.15}$$

Moreover, the dependent variables are changed to:

$$\begin{aligned} u^* &= \omega(x,t)F(\eta), & u_w &= u_w(x,t), \\ v^* &= \zeta(x,t)E(\eta), & v_w &= v_w(x,t), \\ {H_1}^* &= \Gamma(x,t)H(\eta), & H_{1w} &= H_{1w}(x,t), \\ {H_2}^* &= \lambda(x,t)J(\eta), & H_{2w} &= H_{2w}(x,t), \\ C^* &= C^*(\eta), & \theta &= \theta(\eta), \\ N^* &= \psi(x,t)g(\eta), \end{aligned} \tag{3.16}$$

where $\pi(x,t),\ \omega(x,t),\ \zeta(x,t),\ \Gamma(x,t),\ \lambda(x,t),\ u_w(x,t),\ v_w(x,t),\ H_{1w}(x,t),\ H_{2w}(x,t)$, and $\psi(x,t)$ are the unknown functions that will be evaluated throughout the reduction process. The system (2.10)-(2.16) can be formulated as follows:

$$\frac{\omega\frac{\partial u_w}{\partial x}}{\pi v_w \zeta}F + \frac{u_w\omega\frac{\partial \pi}{\partial x}}{\pi^2 v_w \zeta}\eta F' + \frac{u_w\frac{\partial \omega}{\partial x}}{\pi v_w \zeta}F + E' + \frac{E}{\eta} = 0, \tag{3.17}$$

$$\begin{aligned} &\frac{\frac{\partial u_w}{\partial t}}{\frac{\mu_{hnf}}{\rho_{hnf}}u_w\ \pi^2}F + \frac{\frac{\partial \pi}{\partial t}}{\frac{\mu_{hnf}}{\rho_{hnf}}\pi^3}\eta F' + \frac{\frac{\partial \omega}{\partial t}}{\frac{\mu_{hnf}}{\rho_{hnf}}\ \omega\pi^2}F + \frac{\omega\frac{\partial u_w}{\partial x}}{\frac{\mu_{hnf}}{\rho_{hnf}}\pi^2}F^2 + \frac{\omega u_w\frac{\partial \pi}{\partial x}}{\frac{\mu_{hnf}}{\rho_{hnf}}\pi^3}\eta F F' + \frac{u_w\frac{\partial \omega}{\partial x}}{\frac{\mu_{hnf}}{\rho_{hnf}}\ \pi^2}\ F^2 \\ &+ \frac{\zeta v_w}{\frac{\mu_{hnf}}{\rho_{hnf}}\pi}EF' - F'' - \frac{1}{\eta}F' + \frac{\sigma B_0^2}{\mu_{hnf}\ \pi^2}F - \frac{\beta g(\Delta T)}{\frac{\mu_{hnf}}{\rho_{hnf}}u_w\ \omega\pi^2}\theta + \frac{(\rho_p-\rho_f)g(\Delta C)}{\mu_{hnf}u_w\ \omega\pi^2}C^* \\ &+ \frac{(\rho_m-\rho_f)g(\Delta N)}{\mu_{hnf}u_w\ \omega\pi^2}N^* - \frac{\mu_e\lambda H_{2w}\Gamma\frac{\partial H_{1w}}{\partial x}}{4\pi\ \mu_{hnf}u_w\ \omega\pi^2}JH - \frac{\mu_e\lambda H_{2w}H_{1w}\Gamma\frac{\partial \pi}{\partial x}}{4\pi\ \mu_{hnf}u_w\ \omega\pi^3}\eta JH' - \frac{\mu_e\lambda H_{2w}H_{1w}\frac{\partial \Gamma}{\partial x}}{4\pi\ \mu_{hnf}u_w\ \omega\pi^2}JH \\ &- \frac{\mu_e\lambda H_{2w}H_{1w}\Gamma}{4\pi\ \mu_{hnf}u_w\ \omega\pi}JH' = 0. \end{aligned} \tag{3.18}$$

$$\begin{aligned} &\frac{\frac{\partial \pi}{\partial t}}{\alpha_{hnf}\pi^3}\theta'\eta + \frac{\omega u_w\frac{\partial \pi}{\partial x}}{\alpha_{hnf}\pi^3}\ F\theta'\eta + \frac{\zeta v_w}{\alpha_{hnf}\pi}E\theta' - \theta'' - \frac{\theta'}{\eta} - \frac{1}{\Delta T K_{hnf}}\mu_{hnf}\left(u_w\omega\right)^2\left(F'\right)^2 \\ &- \frac{\sigma B_0^2\left(\omega u_w\right)^2}{\Delta T k_{hnf}\pi^2}(F)^2 + \frac{\frac{1}{\left(\rho c_p\right)_{hnf}}\left(\frac{16\sigma^* T_\infty^3}{3k^*}\right)}{\alpha_{hnf}}\theta'' + \frac{\frac{1}{\left(\rho c_p\right)_{hnf}}\left(\frac{16\sigma^* T_\infty^3}{3k^*}\right)}{\alpha_{hnf}}\frac{\theta'}{\eta} - \frac{\tau\frac{D_T}{T_\infty}\Delta T}{\alpha_{hnf}}\left(\theta'\right)^2 \\ &- \frac{\tau D_B}{\alpha_{hnf}}\theta' C^{*'} - \frac{\frac{Q_0}{\left(\rho c_p\right)_{hnf}}}{\alpha_{hnf}\pi^2}\theta = 0, \end{aligned} \tag{3.19}$$

$$\frac{\frac{\partial \pi}{\partial t}}{D_B\pi^3}\eta C^{*'} + \frac{\omega u_w\frac{\partial \pi}{\partial x}}{D_B\pi^3}\eta C^{*'}F + \frac{\zeta v_w}{D_B\pi}EC^{*'} - C^{*''} - \frac{\frac{D_T}{T_\infty}\Delta T}{D_B}\theta'' = 0, \tag{3.20}$$

$$\frac{\frac{\partial\pi}{\partial t}}{D_n\pi^3}\eta g' + \frac{\frac{\partial\psi}{\partial t}}{D_n\psi\pi^2}g + \frac{\omega u_w\frac{\partial\pi}{\partial x}}{D_n\pi^3}\eta g'F + \frac{\omega u_w\frac{\partial\psi}{\partial x}}{D_n\psi\pi^2}Fg + \frac{\zeta v_w}{D_n\pi}Eg' + \frac{bw_c}{D_n}gC^{*''} + \frac{bw_c\frac{N_\infty}{\Delta N}}{D_n\psi}C^{*''} + \frac{bw_c}{D_n}C^{*'}g' - g'' = 0, \tag{3.21}$$

$$\frac{\frac{\partial H_{1_w}}{\partial t}}{\eta_0 H_{1w}\,\pi^2}H + \frac{\frac{\partial\pi}{\partial t}}{\eta_0\,\pi^3}\eta H' + \frac{\frac{\partial\Gamma}{\partial t}}{\eta_0\,\Gamma\pi^2}H + \frac{\omega u_w\frac{\partial H_{1_w}}{\partial x}}{\eta_0 H_{1w}\,\pi^2}FH + \frac{\omega u_w\frac{\partial\pi}{\partial x}}{\eta_0\,\pi^3}F\eta H' + \frac{\omega u_w\frac{\partial\Gamma}{\partial x}}{\eta_0\,\Gamma\pi^2}FH + \frac{\zeta v_w}{\eta_0\,\pi}EH' - H'' - \frac{H'}{\eta} = 0, \tag{3.22}$$

$$\frac{\frac{\partial H_{2_w}}{\partial t}}{\eta_0 H_{2w}\,\pi^2}J + \frac{\frac{\partial\pi}{\partial t}}{\eta_0\,\pi^3}J'\eta + \frac{\frac{\partial\Gamma}{\partial t}}{\eta_0\,\lambda\pi^2}J + \frac{\omega u_w\frac{\partial H_{2_w}}{\partial x}}{\eta_0 H_{2w}\,\pi^2}FJ + \frac{\omega u_w\frac{\partial\pi}{\partial x}}{\eta_0\,\pi^3}\eta FJ' + \frac{\omega u_w\frac{\partial\Gamma}{\partial x}}{\eta_0\,\lambda\pi^2}FJ + \frac{\zeta v_w}{\eta_0\,\pi}EJ' - J'' - \frac{J'}{\eta} = 0, \tag{3.23}$$

where $\Delta T = T_w - T_\infty, \Delta C = C_w - C_\infty, \Delta N = N_w - N_\infty$. Dashes are used to represent derivatives with regard to η. The following relations must be followed to properly turn the equations (3.17)-(3.23) into an ODE system:

$$A_1 = \frac{\omega\frac{\partial u_w}{\partial x}}{\pi v_w\zeta},\quad A_2 = \frac{u_w\omega\frac{\partial\pi}{\partial x}}{\pi^2 v_w\zeta},\quad A_3 = \frac{u_w\frac{\partial\omega}{\partial x}}{\pi v_w\zeta},\quad A_4 = \frac{\frac{\partial u_w}{\partial t}}{\frac{\mu_{hnf}}{\rho_{hnf}}u_w\,\pi^2},\quad A_5 = \frac{\frac{\partial\pi}{\partial t}}{\frac{\mu_{hnf}}{\rho_{hnf}}\pi^3},\quad A_6 = \frac{\frac{\partial\omega}{\partial t}}{\frac{\mu_{hnf}}{\rho_{hnf}}\,\omega\pi^2},$$
$$A_7 = \frac{\omega\frac{\partial u_w}{\partial x}}{\frac{\mu_{hnf}}{\rho_{hnf}}\pi^2},\quad A_8 = \frac{\omega u_w\frac{\partial\pi}{\partial x}}{\frac{\mu_{hnf}}{\rho_{hnf}}\pi^3},\quad A_9 = \frac{u_w\frac{\partial\omega}{\partial x}}{\frac{\mu_{hnf}}{\rho_{hnf}}\pi^2},\quad A_{10} = \frac{\zeta v_w}{\frac{\mu_{hnf}}{\rho_{hnf}}\pi},\quad A_{11} = \frac{\sigma B_0^2}{\mu_{hnf}\,\pi^2},$$
$$A_{12} = \frac{\beta g(\Delta T)}{\frac{\mu_{hnf}}{\rho_{hnf}}u_w\,\omega\pi^2},\quad A_{13} = \frac{(\rho_p-\rho_f)g(\Delta C)}{\mu_{hnf}u_w\,\omega\pi^2},\quad A_{14} = \frac{(\rho_m-\rho_f)g(\Delta N)}{\mu_{hnf}u_w\,\omega\pi^2},$$
$$A_{15} = \frac{\mu_e\lambda H_{2w}\Gamma\frac{\partial H_{1w}}{\partial x}}{4\pi\,\mu_{hnf}u_w\,\omega\pi^2}, A_{16} = \frac{\mu_e\lambda H_{2w}H_{1w}\Gamma\frac{\partial\pi}{\partial x}}{4\pi\,\mu_{hnf}u_w\,\omega\pi^3},\quad A_{17} = \frac{\mu_e\lambda H_{2w}H_{1w}\frac{\partial\Gamma}{\partial x}}{4\pi\,\mu_{hnf}u_w\,\omega\pi^2},$$
$$A_{18} = \frac{\mu_e\lambda H_{2w}H_{1w}\Gamma}{4\pi\,\mu_{hnf}u_w\,\omega\pi}, A_{19} = \frac{\frac{\partial\pi}{\partial t}}{\alpha_{hnf}\pi^3}, A_{20} = \frac{\omega u_w\frac{\partial\pi}{\partial x}}{\alpha_{hnf}\pi^3},\quad A_{21} = \frac{\zeta v_w}{\alpha_{hnf}\pi},$$
$$A_{22} = \frac{1}{\Delta T K_{hnf}}\mu_{hnf}\left(u_w\omega\right)^2,\quad A_{23} = \frac{\sigma B_0^2\left(\omega u_w\right)^2}{\Delta T k_{hnf}\pi^2}, A_{24} = \frac{\frac{Q_0}{\left(\rho c_p\right)_{hnf}}}{\alpha_{hnf}\pi^2},\quad A_{25} = \frac{\frac{\partial\pi}{\partial t}}{D_B\pi^3},$$
$$A_{26} = \frac{\omega u_w\frac{\partial\pi}{\partial x}}{D_B\pi^3}, A_{27} = \frac{\zeta v_w}{D_B\pi},\quad A_{28} = \frac{\frac{\partial\pi}{\partial t}}{D_n\pi^3},\quad A_{29} = \frac{\frac{\partial\psi}{\partial t}}{D_n\psi\pi^2},\quad A_{30} = \frac{\omega u_w\frac{\partial\pi}{\partial x}}{D_n\pi^3},\quad A_{31} = \frac{\omega u_w\frac{\partial\psi}{\partial x}}{D_n\psi\pi^2},$$
$$A_{32} = \frac{\zeta v_w}{D_n\pi},\quad A_{33} = \frac{bw_c\frac{N_\infty}{\Delta N}}{D_n\psi},\quad A_{34} = \frac{\frac{\partial H_{1w}}{\partial t}}{\eta_0 H_{1w}\,\pi^2},\quad A_{35} = \frac{\frac{\partial\pi}{\partial t}}{\eta_0\,\pi^3},\quad A_{36} = \frac{\frac{\partial\Gamma}{\partial t}}{\eta_0\,\Gamma\pi^2},\quad A_{37} = \frac{\omega u_w\frac{\partial H_{1w}}{\partial x}}{\eta_0 H_{1w}\,\pi^2},$$
$$A_{38} = \frac{\omega u_w\frac{\partial\pi}{\partial x}}{\eta_0\,\pi^3},\quad A_{39} = \frac{\omega u_w\frac{\partial\Gamma}{\partial x}}{\eta_0\,\Gamma\pi^2},\quad A_{40} = \frac{\zeta v_w}{\eta_0\,\pi},\quad A_{41} = \frac{\frac{\partial H_{2w}}{\partial t}}{\eta_0 H_{2w}\,\pi^2},\quad A_{42} = \frac{\frac{\partial\pi}{\partial t}}{\eta_0\,\pi^3},$$
$$A_{43} = \frac{\frac{\partial\Gamma}{\partial t}}{\eta_0\,\lambda\pi^2},\quad A_{44} = \frac{\omega u_w\frac{\partial H_{2w}}{\partial x}}{\eta_0 H_{2w}\,\pi^2},\quad A_{45} = \frac{\omega u_w\frac{\partial\pi}{\partial x}}{\eta_0\,\pi^3},\quad A_{46} = \frac{\omega u_w\frac{\partial\Gamma}{\partial x}}{\eta_0\,\lambda\pi^2},\quad A_{47} = \frac{\zeta v_w}{\eta_0\,\pi}. \tag{3.24}$$

Similarly, formulae (3.17)-(3.23) enable the following analysis-based conclusions to be drawn:

$$\pi = c_1,\ u_w = c_4 e^{c_1^2 c_2 t},\ \omega = c_5 e^{-c_1^2 c_2 t},\ \psi = c_8, H_{1w} = c_9 e^{c_1^2 c_{14} t},\ \Gamma = c_{10} e^{-c_1^2 c_{14} t},$$
$$H_{2w} = c_{11} e^{c_1^2 c_{15} t},\ \lambda = c_{12} e^{-c_1^2 c_{15} t},\ \zeta v_w = c_7. \tag{3.25}$$

The final form of the ODE system is shown below:

$$E^{'} + \frac{E}{\eta} = 0, \tag{3.26}$$

$$\frac{c_7}{\frac{\mu_{hnf}}{\rho_{hnf}} c_1} E F^{'} - F^{''} - \frac{1}{\eta} F^{'} + \frac{\sigma B_0^2}{\mu_{hnf}\ {c_1}^2} F - \frac{\beta g(\Delta T)}{\frac{\mu_{hnf}}{\rho_{hnf}} c_5\ c_4 {c_1}^2}\theta + \frac{(\rho_p - \rho_f) g(\Delta C)}{\mu_{hnf} c_5\ c_4 {c_1}^2} C^*$$
$$+ \frac{(\rho_m - \rho_f) g(\Delta N)}{\mu_{hnf} c_5\ c_4 {c_1}^2} c_8 g\ - \frac{\mu_e c_9\ c_{10} c_{11} c_{12}}{4\pi\ \mu_{hnf} c_5\ c_4 c_1} J H^{\prime} = 0, \tag{3.27}$$

$$\frac{c_7}{\alpha_{hnf} c_1} E\theta^{'} - \theta^{''} - \frac{\theta^{'}}{\eta} - \frac{1}{\Delta T K_{hnf}} \mu_{hnf}\ (c_5\ c_4)^2 \left(F^{'}\right)^2 - \frac{\sigma B_0^2\ (c_5\ c_4)^2}{\Delta T k_{hnf}\ {c_1}^2} (F)^2 + \frac{\frac{1}{(\rho c_p)_{hnf}} \left(\frac{16\sigma^* T_\infty^3}{3k^*}\right)}{\alpha_{hnf}} \theta^{''}$$
$$+ \frac{\frac{1}{(\rho c_p)_{hnf}} \left(\frac{16\sigma^* T_\infty^3}{3k^*}\right)}{\alpha_{hnf}} \frac{\theta^{'}}{\eta} - \frac{\tau \frac{D_T}{T_\infty} \Delta T}{\alpha_{hnf}} \left(\theta^{'}\right)^2 - \frac{\tau D_B}{\alpha_{hnf}} \theta^{'} C^{*^{'}} - \frac{\frac{Q_0}{(\rho c_p)_{hnf}}}{\alpha_{hnf}\ {c_1}^2} \theta = 0, \tag{3.28}$$

$$\frac{c_7}{D_B c_1} E C^{*^{'}} - C^{*^{''}} - \frac{\frac{D_T}{T_\infty} \Delta T}{D_B} \theta^{''} = 0, \tag{3.29}$$

$$\frac{c_7}{D_n c_1} E g^{\prime} + \frac{b w_c}{D_n} g C^{*^{''}} + \frac{b w_c \frac{N_\infty}{\Delta N}}{D_n c_8} C^{*^{''}} + \frac{b w_c}{D_n} C^{*^{'}} g^{\prime} - g^{''} = 0, \tag{3.30}$$

$$\frac{c_7}{\eta_0\ c_1} E H^{\prime} - H^{\prime\prime} - \frac{H^{\prime}}{\eta} = 0, \tag{3.31}$$

$$\frac{c_7}{\eta_0\ c_1} E J^{\prime} - J^{\prime\prime} - \frac{J^{\prime}}{\eta} = 0. \tag{3.32}$$

The boundary condition are changed to:

$$\begin{aligned} &At \quad r = R(x), \\ &F = 1,\ E = 0,\ H = 1,\ J = 1,\ \theta = 1,\ \ C^* = 1,\ \ g = 1, \\ &At \quad r \to \infty, \\ &F = 0,\ H = 0,\ J = 0,\ \ \theta = 0,\ \ C^* = 0,\ \ g = 0. \end{aligned} \tag{3.33}$$

The following relationships, however, are used to get the nanofluid parameters.

$$\mu_{hnf} = \frac{\mu_f}{(1-\phi_{n1})^{2.5} (1-\phi_{n2})^{2.5} (1-\phi_{n3})^{2.5}}, \tag{3.34}$$

$$\rho_{hnf} = \rho_f \left[(1-\phi_{n1}) \left((1-\phi_{n2}) \left[(1-\phi_{n3}) \rho_f + \phi_{n3} \rho_{n3}\right] + \phi_{n2} \rho_{n2}\right) + \phi_{n1} \rho_{n1}\right], \tag{3.35}$$

$$(\rho c_p)_{hnf} = (\rho c_p)_f \left[(1-\phi_{n1}) \left((1-\phi_{n2}) \left[(1-\phi_{n3}) (\rho c_p)_f + \phi_{n3} (\rho c_p)_3\right] + \phi_{n2} (\rho c_p)_2\right) + \phi_{n1} (\rho c_p)_1\right], \tag{3.36}$$

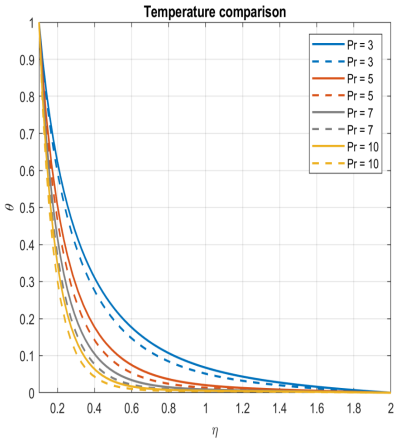

FIGURE 2. Pr temperature comparison. solid for Ahmad et al. [1], dashed lines for current investigation.

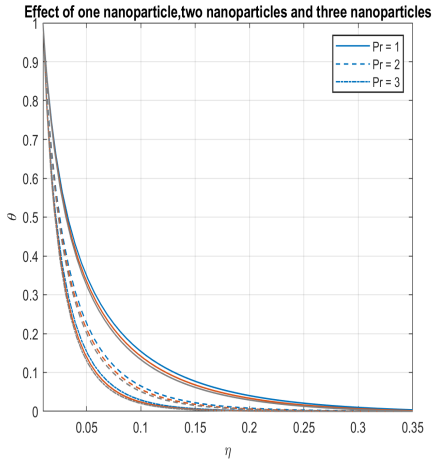

FIGURE 3. The influence of different number of nanoparticles.

$$k_{hnf} = k_f \left(\frac{k_{n1} + (n-1)k_f - (n-1)\phi_{n1}\,(k_f - k_{n1})}{k_{n1} + (n-1)k_f + \phi_{n1}\,(k_f - k_{n1})} \right) \left(\frac{k_{n2} + (n-1)k_f - (n-1)\phi_{n2}\,(k_f - k_{n2})}{k_{n2} + (n-1)k_f + \phi_{n2}\,(k_f - k_{n2})} \right) \tag{3.37}$$

$$\left(\frac{k_{n3} + (n-1)k_f - (n-1)\phi_{n3}\,(k_f - k_{n3})}{k_{n3} + (n-1)k_f + \phi_{n3}\,(k_f - k_{n3})} \right). \tag{3.38}$$

4. Results and Discussion

Equations (3.26)-(3.32), which are subjected to the boundary conditions in (3.33), are numerically solved using the MATLAB package using Runge-Kutta procedure and the shooting technique. The present study looked at the effects of several factors, including Prandtl number, Pr, Brownian motion coefficient, D_B, Thermophoresis diffusion coefficient, D_T, microorganism diffusion coefficient, D_n, concentration difference, δc,temperature difference, δt , Schmidt number, Sc, bioconvection Peclet number, Pe , Lewis number,Lb , and magnetic diffusivity, η_0.

4.1. Validation of the obtained results.

The updated outcomes are checked out with those of Ahmad et al. [1] for validation reasons. The influence of Prandtl number Pr, which was employed as a measure of comparison showing a high level of agreement, as depicted in Figure 2. Moreover, the impact of employing one, two, or three nanoparticles is illustrated in Figure 3.

4.2. Convergence of the method and Error Analysis.

Due to the fact that the mathematical model and its invariant system of ODEs have no analytical solution, a reference value of step $h = 0.001$ is used to compare the results with coarser step. The global error at each point is calculated. The reference step value is $h_{ref} = 0.0001$. These results and global errors are illustrated in Tables 1 and 2.

4.3. **Prandtl number's significance.** The Prandtl number is a dimensionless parameter that describes the relative magnitudes of momentum diffusivity (kinematic viscosity) and heat diffusivity in a fluid. The impact of the Prandtl number on many fluid parameters, including velocity, temperature, nanoparticles, and density of bacteria, may be explained as follows:

- Velocity: The Prandtl number impacts the fluid's momentum diffusivity. A higher Prandtl value indicates that momentum diffuses slower than thermal diffusion. As a result, the velocity profiles of the fluid can be altered. For example, a higher Prandtl number fluid has a larger momentum boundary layer, which influences velocity distribution at solid borders or interfaces.

TABLE 1. Compared values at different step values, h.

$\eta \in [0,2]$ using $\eta = 1$				
	$h_3 = 0.025$	$h_2 = 0.05$	$h_1 = 0.1$	$h_{ref} = .0001$
Y2	0.0833	0.0863	0.0849	0.0831
Y3	-0.1507	-0.1554	-0.1532	-0.1504
Y4	0.1300	0.1339	0.1320	0.1298
Y5	-0.1880	-0.1919	-0.1901	-0.1878
Y6	0.5000	0.5101	0.5051	0.5000
Y7	-0.5027	-0.5045	-0.5034	-0.5030
Y	0.0210	0.0220	0.0215	0.0210
Y9	-0.0479	-0.0493	-0.0481	-0.0480
Y10	0.1301	0.1339	0.1321	0.1299
Y11	-0.1929	-0.2012	-0.1931	-0.1930
Y12	0.1301	0.1339	0.1321	0.1299
Y13	-0.1881	-0.1919	-0.1901	-0.1878

TABLE 2. The global error of each variable.

$\eta \in [0,2]$ using $\eta = 1$			
	$h_3 = 0.025$	$h_2 = 0.05$	$h_1 = 0.1$
Error in Y2	0.0002	0.0032	0.0018
Error in Y3	0.0003	0.0050	0.0028
Error in Y4	0.0002	0.0041	0.0022
Error in Y5	0.0002	0.0041	0.0023
Error in Y6	0.0000	0.0101	0.0051
Error in Y7	0.0003	0.0015	0.0004
Error in Y8	0.0000	0.001	0.0005
Error in Y9	0.0001	0.0013	0.0001
Error in Y10	0.0002	0.004	0.0022
Error in Y11	0.0001	0.0082	0.0001
Error in Y12	0.0002	0.004	0.0022
Error in Y13	0.0003	0.0023	0.0023

- Temperature: Thermal diffusivity is the main factor that influences the Prandtl number. Thermal diffusion is thought to be slower than momentum diffusion when the Prandtl number is larger. As such, the Prandtl number can have an impact on the fluid's temperature profiles. Fluids with a higher Prandtl number often have slower heat transfer rates and a more noticeable temperature boundary layer.
- Nanoparticles: The behavior of suspended nanoparticles in a fluid is indirectly influenced by the Prandtl number. The temperature distribution and, thus, the thermal energy transfer to the nanoparticles can be influenced by the Prandtl number. As such, the temperature field can affect the nanoparticles' Brownian motion, propensity to aggregate or disperse, and interaction with the surrounding fluid.
- Density of bacteria: The Prandtl number affects temperature, which in turn affects fluid density indirectly. The fluid's thermal expansion or contraction may be influenced by the Prandtl number, which also has an impact on temperature profiles. Temperature distribution variations can result in equivalent changes in fluid density, which can have an impact on buoyancy effects, density-driven flows, and the general behavior of fluid flow. These observations are shown in Figures 4-10.

4.4. **The significance of Brownian motion coefficient D_B.**

The diffusion of particles or molecules caused by Brownian motion is measured by the Brownian motion coefficient, often known as D_B. It is affected by a number of variables, such as temperature and density, and measures the random movement of particles floating in a fluid media, such as bacteria or nanoparticles. For particles moving in a Brownian motion, the velocity and the Brownian motion coefficient are inversely correlated. Particles diffuse faster with increasing D_B, leading to greater velocities. Brownian motion is also essential to the behavior of nanoparticles in suspension. The rate of dispersion and diffusion of nanoparticles in a fluid medium are determined by the Brownian motion coefficient. Increased dispersion and a more even dispersion of nanoparticles are caused by higher $D_B$values. This feature is frequently used in applications like medication delivery, where the motion of the particles affects how they are transported and targeted inside biological systems. Figures 11-17 illustrate these observations.

4.5. **Thermophoresis diffusion coefficient's significance.**

The Thermophoresis diffusion coefficient, D_T, influences various elements including velocity, nanoparticles, and bacterial density. Let's investigate the relevance of this coefficient in each of these cases.

- Velocity: Thermophoresis is the mobility of particles in a fluid caused by a temperature differential. The Thermophoresis diffusion coefficient governs the magnitude of this movement. A greater diffusion coefficient means a stronger thermophoretic action, which leads to faster particle speeds. A smaller diffusion coefficient, on the other hand, results in weaker thermophoretic motion and slower particle velocities.
- Nanoparticles: Thermophoresis is widely used in the research and manipulation of nanoparticles. The diffusion coefficient plays an important role in defining nanoparticle behavior in thermophoretic environments. It changes the pace at which nanoparticles move in response to a temperature gradient, hence influencing their spatial distribution and concentration profiles.
- Bacterial Density: The Thermophoresis diffusion coefficient indicates the quantity of bacterial mobility caused by a temperature difference. Bacterial cells can show thermophoretic behavior, which influences their geographic distribution and population dynamics. The diffusion coefficient impacts the rate at which bacteria travel over a thermal gradient. Figures 18–23 illustrate these observations.

4.6. **The significance of the microorganism diffusion coefficient D_n.**

The microorganism diffusion coefficient, D_n, is critical in measuring the velocity and density of bacteria in fluids. Let's explore how this coefficient affects these parameters.

- Velocity: The velocity at which bacteria move through fluids is directly influenced by the microorganism diffusion coefficient. The velocity of diffusion is inversely related to the diffusion coefficient and proportionate to the concentration gradient, as per Fick's law of diffusion. As a result, microorganisms in the fluid diffuse more quickly and move at higher velocities when the diffusion coefficient is larger. Higher D_n values allow bacteria to travel through the fluid more quickly, which facilitates their movement and dispersion.
- Density: The density of bacteria in fluids is also influenced by the microorganism diffusion coefficient. Population growth and dispersal are balanced to determine the density of bacteria. Bacteria can spread more readily across the fluid with a greater diffusion coefficient, which can lead to a more homogenous distribution and possibly lower local densities. On the other hand, a reduced diffusion coefficient limits the spread of germs, increasing local concentrations in certain fluid zones. Figures 24-27 illustrate these observations.

4.7. **The significance of concentration difference, δc.**

The concentration difference, or gradient, has a substantial impact on a variety of fluid properties, including velocity and temperature. Let's investigate the consequences of concentration differences in each of these contexts:

- Velocity: A concentration difference in fluid flow can cause particles, including bacteria, to move through a process known as advection. When there is a concentration gradient in a fluid, particles tend to migrate from high concentration to low concentration areas. This movement causes the particles to travel at an advection velocity. A bigger concentration difference often results in a higher advection velocity since the driving force for particle motion is greater. As a result, an increasing concentration differential often correlates to higher bacterial velocities in the fluid.

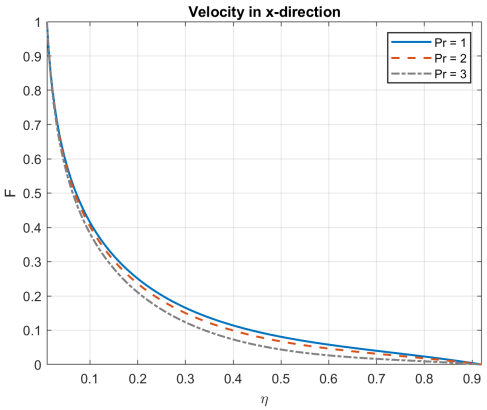

FIGURE 4. The influence of Pr on velocity in x-direction.

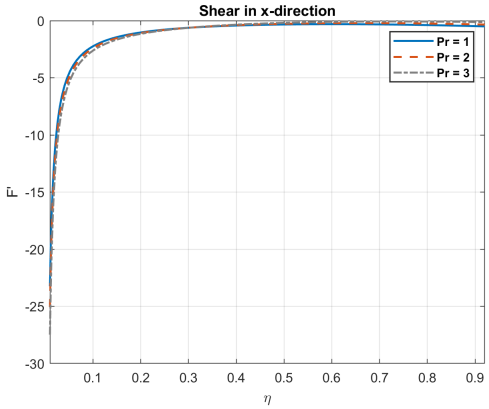

FIGURE 5. The influence of Pr on shear stress in x-direction.

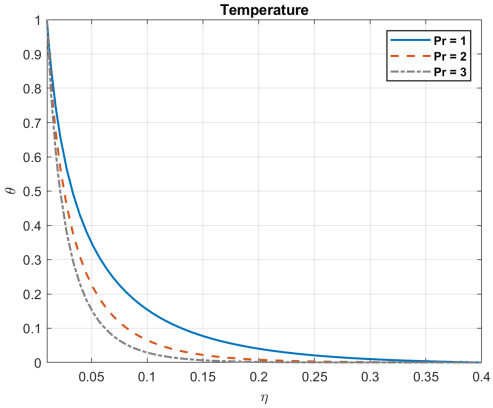

FIGURE 6. The influence of Pr on temperature.

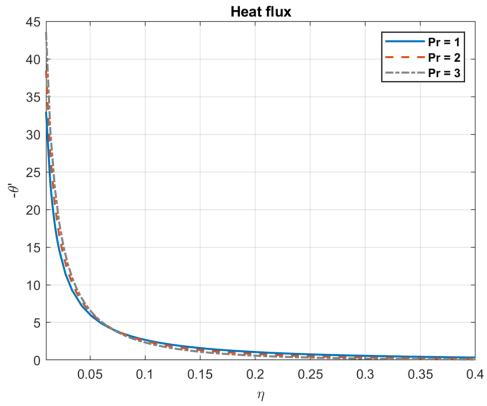

FIGURE 7. The influence of Pr on heat flux.

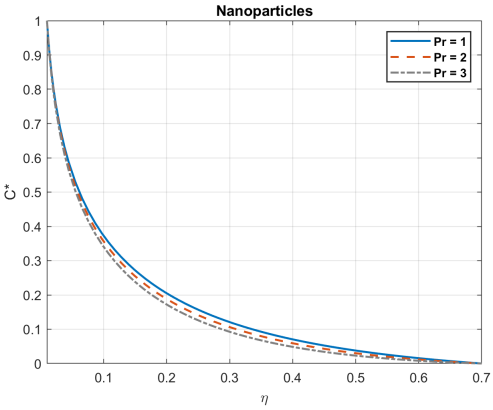

FIGURE 8. The influence of Pr on nanoparticles concentration.

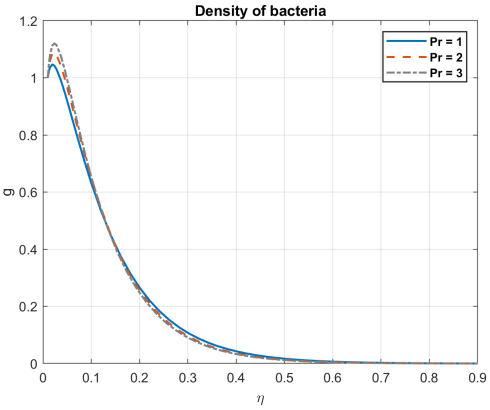

FIGURE 9. The influence of Pr on density of bacteria.

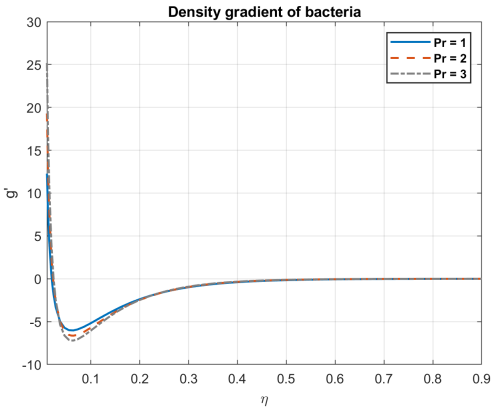

FIGURE 10. The influence of Pr on density gradient of bacteria.

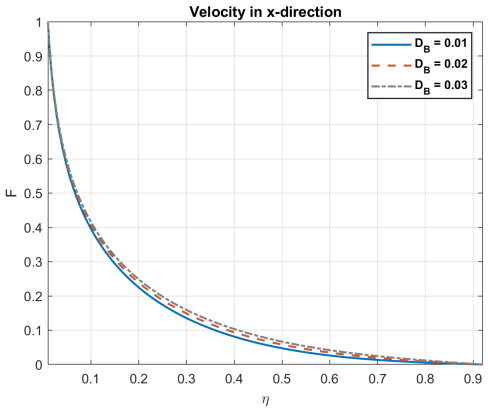

FIGURE 11. The influence of D_B on velocity in x-direction.

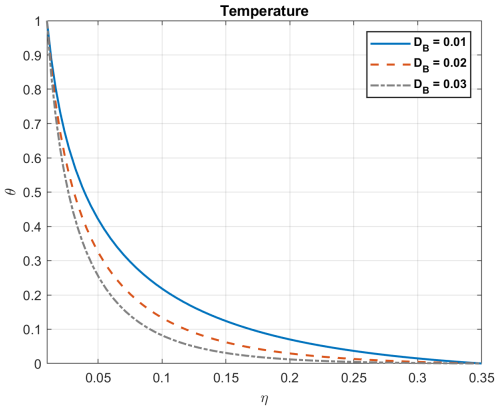

FIGURE 12. The influence of D_B on temperature.

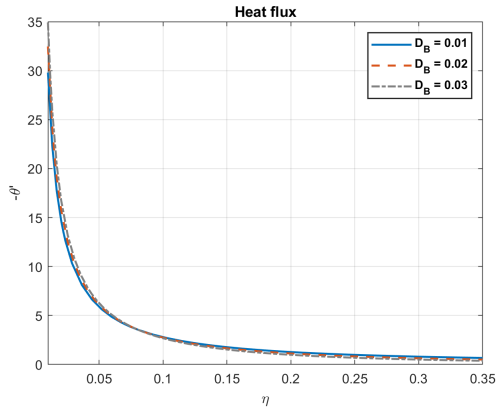

FIGURE 13. The influence of D_B on heat flux.

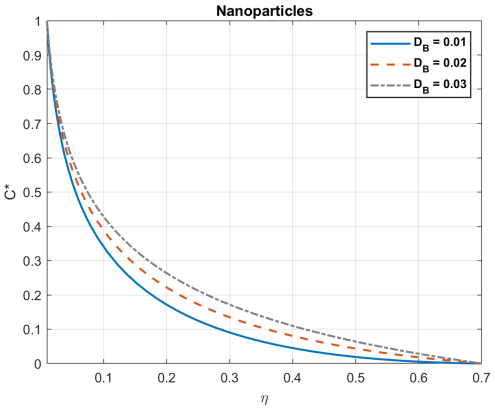

FIGURE 14. The influence of D_B on nanoparticles concentration.

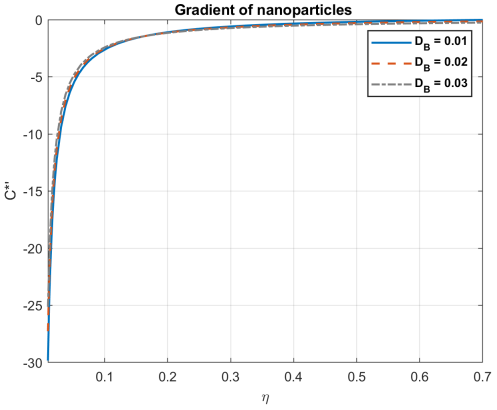

FIGURE 15. The influence of D_B on gradient of nanoparticles concentration.

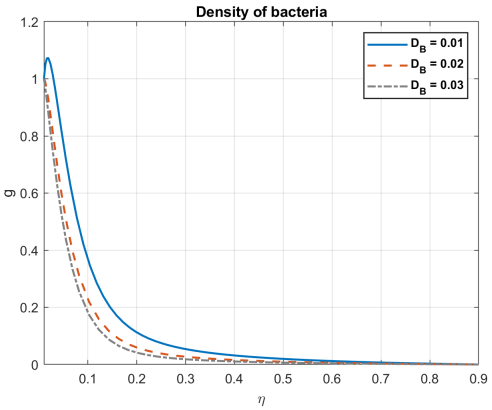

FIGURE 16. The influence of D_B on density of bacteria.

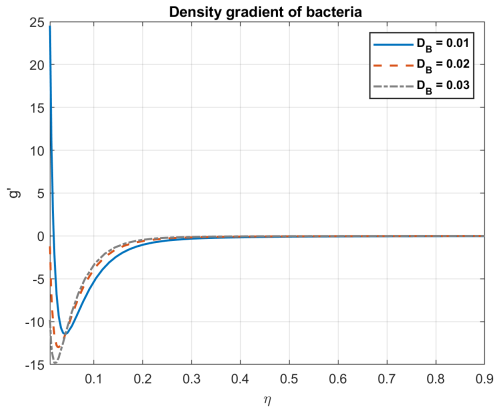

FIGURE 17. The influence of D_B on density gradient of bacteria.

- Temperature: The concentration difference can also affect the temperature distribution in a fluid. A concentration gradient can sometimes cause a temperature gradient as a result of fluid dynamics. Figures 28-31 illustrate these observations.

4.8. The significance of temperature difference ratio, δT.

- Velocity: A temperature difference in fluid dynamics can cause fluid movement through a process known as thermally induced convection. When there is a temperature difference in a fluid, its density changes owing to thermal expansion or contraction. This density differential causes fluid motion, resulting in velocity. The magnitude of the temperature differences has a direct impact on the intensity of the convective flow, with bigger temperatures resulting in higher velocities.
- Temperature: The fluid's internal temperature distribution is immediately impacted by the temperature difference. Variations in temperature throughout the fluid might result from a steeper temperature gradient, which is correlated with a larger temperature difference. Conduction and convection are two heat transmission mechanisms that can be fueled by a temperature difference and affect a fluid's total temperature. Figures 32-33 illustrate these observations.

4.9. The significance of Schmidt number, Sc.

The Schmidt number (Sc) is a dimensionless quantity that describes the relevance of momentum and mass transfer in fluid systems. It compares the rates of molecular diffusion of momentum (kinematic viscosity) and mass (mass diffusivity). The effect of Schmidt number on velocity and bacterial density in fluids may be characterized as follows:

- Velocity: The Schmidt number influences the velocity of fluid flow during mass transfer. Higher Schmidt numbers imply a slower rate of mass diffusion relative to momentum diffusion. When mass transfer is slower than momentum transfer (high Sc), fluid flow is dominated by velocity-driven processes. In systems where mass diffusion is quicker than momentum diffusion (low Sc), mass-driven processes have a greater effect on fluid flow. As a result, the Schmidt number has an effect on fluid flow velocity by influencing the relative significance of momentum and mass transfer.
- Bacterial Density: The Schmidt number's effect on bacterial density is determined by a variety of factors such as bacterial motility, growth, and mass transfer processes. In high-Sc systems, where momentum diffusion takes precedence over mass diffusion, bacterial density can be controlled by fluid flow pattern as well as nutrition and oxygen supply. Figures 34-37 illustrate these observations.

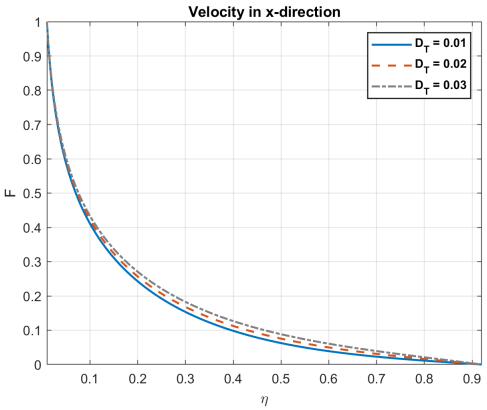

FIGURE 18. The influence of D_T on velocity in x-direction.

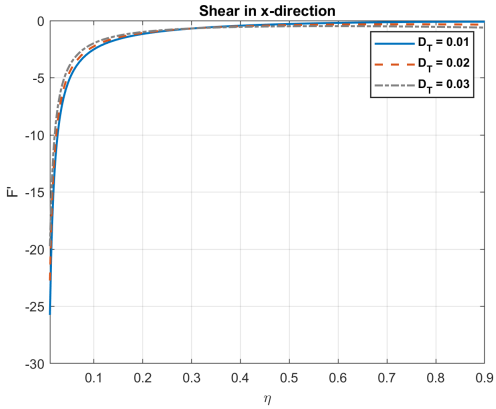

FIGURE 19. The influence of D_T on shear stress in x-direction.

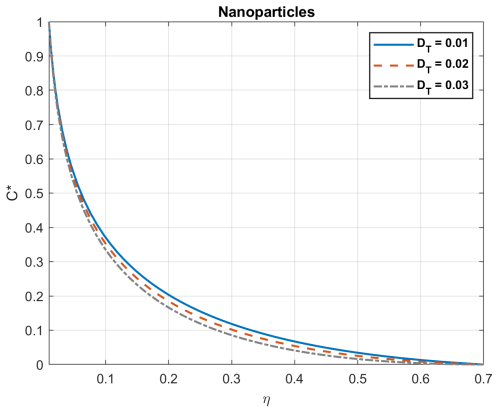

FIGURE 20. The influence of D_T on nanoparticles concentration.

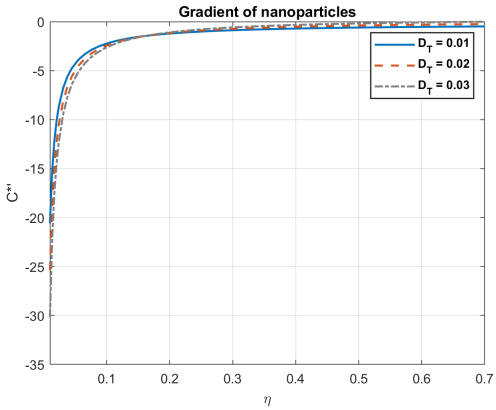

FIGURE 21. The influence of D_T on gradient of nanoparticles concentration.

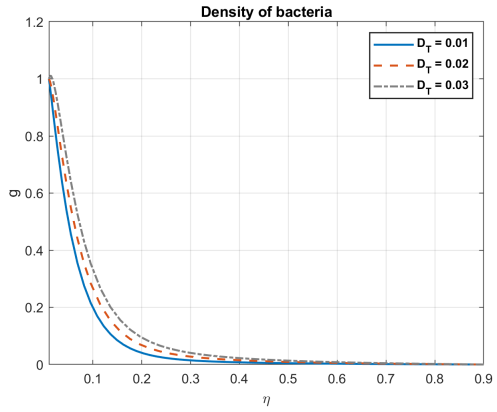

FIGURE 22. The influence of D_T on density of bacteria.

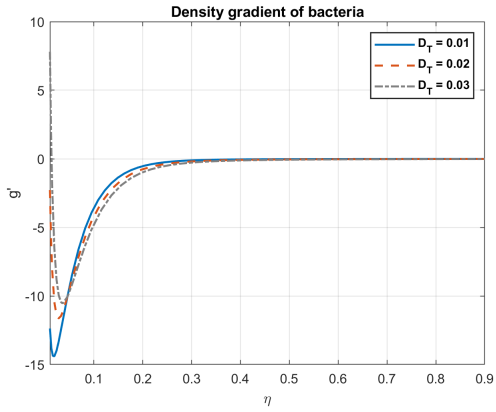

FIGURE 23. The influence of D_T on density gradient of bacteria.

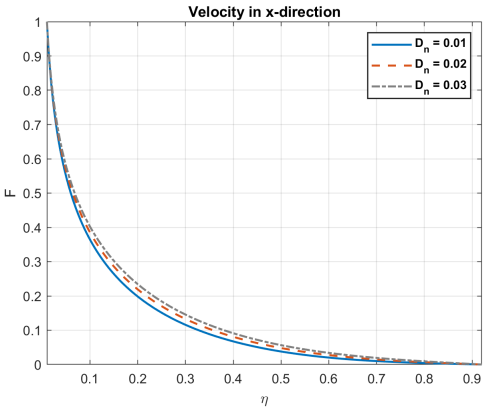

FIGURE 24. The influence of D_n on velocity in x-direction.

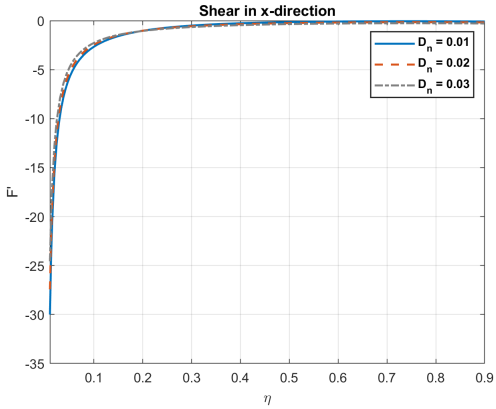

FIGURE 25. The influence of D_n on shear stress in x-direction.

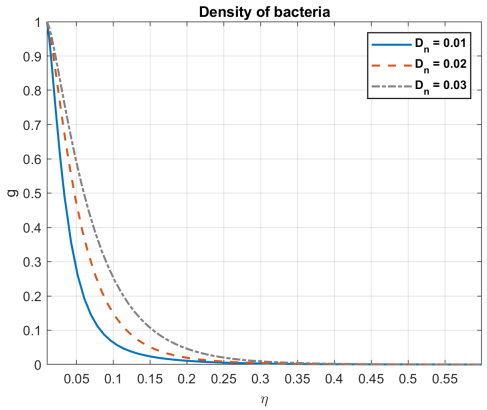

FIGURE 26. The influence of D_n on density of bacteria.

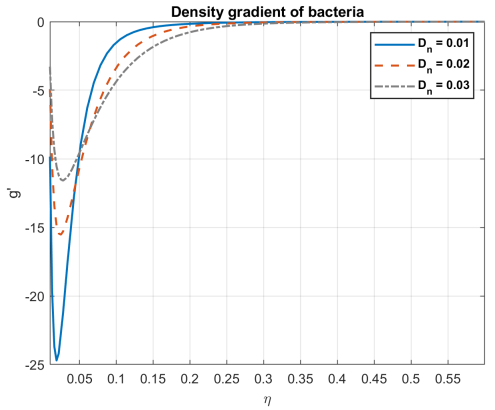

FIGURE 27. The influence of D_n on density gradient of bacteria.

4.10. **The significance of Peclet number,** Pe**.**

The Peclet number (Pe) is a dimensionless metric that describes the relative significance of convective vs diffusive transport in fluid systems. It connects the rates of convective transport (advection) to those of diffusive transport (molecular diffusion). The effect of Peclet number on velocity, temperature, nanoparticles, and bacterial density in fluids may be characterized as follows:

- Velocity: The Peclet number has a direct effect on fluid velocity. A higher Peclet number indicates that convective transport (advection) is more dominant than diffusive transport (molecular diffusion). In high-Pe systems, convective transport is the dominant cause of fluid motion, whereas advection dominates fluid flow. Figure 38 illustrate these observations.

4.11. **The significance of Lewis number** Lb**.**

The Lewis number affects the behavior of fluids containing nanoparticles and is mostly utilized in the research of transport phenomena including heat and mass transfer. In particular, the Lewis number can affect a fluid's nanoparticle dispersion and velocity as follows:

Through its impact on the heat and mass diffusivities, the Lewis number influences the velocity of nanoparticles in a fluid. When compared to mass diffusion, heat diffusion is more prevalent when the Lewis number is larger.

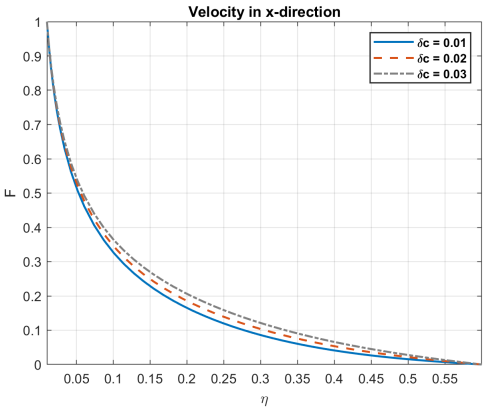

FIGURE 28. The influence of δc on velocity in x-direction.

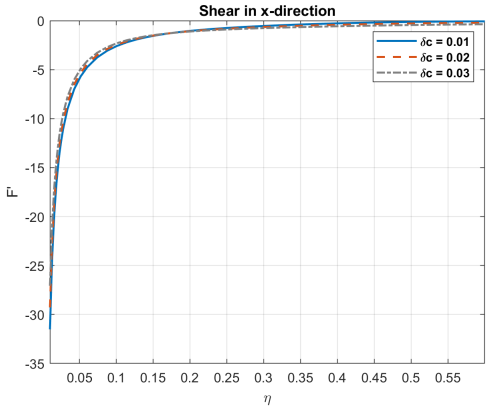

FIGURE 29. The influence of δc on shear stress in x-direction.

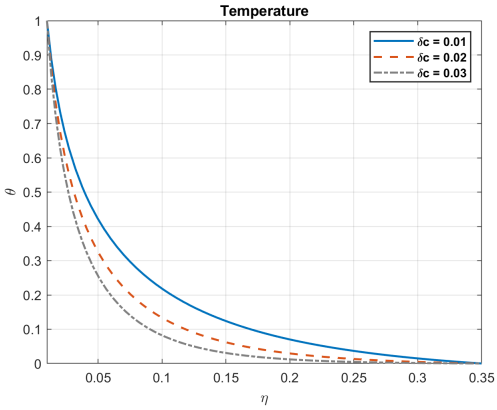

FIGURE 30. The influence of δc on temperature.

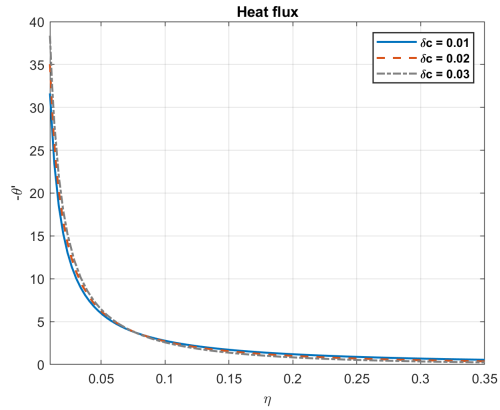

FIGURE 31. The influence of δc on heat flux.

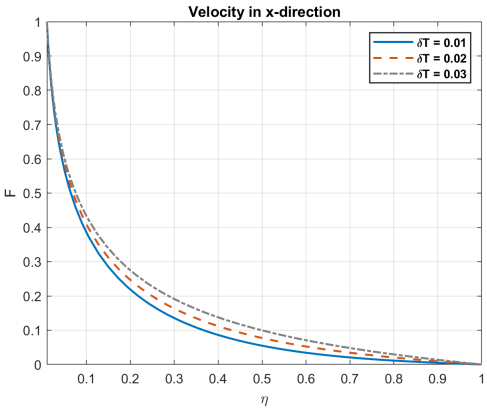

FIGURE 32. The influence of δT on velocity in x-direction.

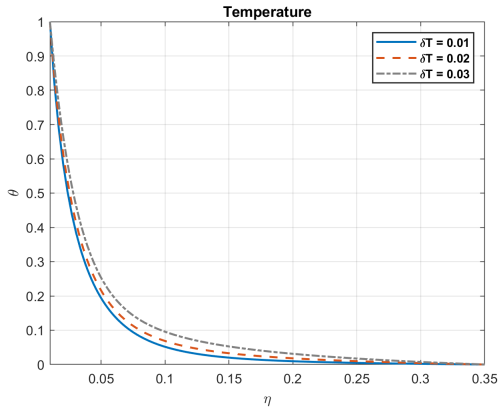

FIGURE 33. The influence of δT on temperature.

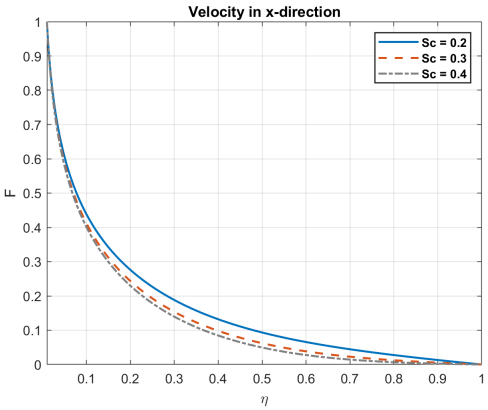

FIGURE 34. The influence of Sc on velocity in x-direction.

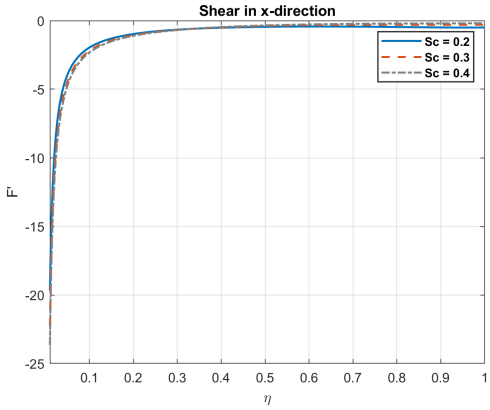

FIGURE 35. The influence of Sc on shear stress in x-direction.

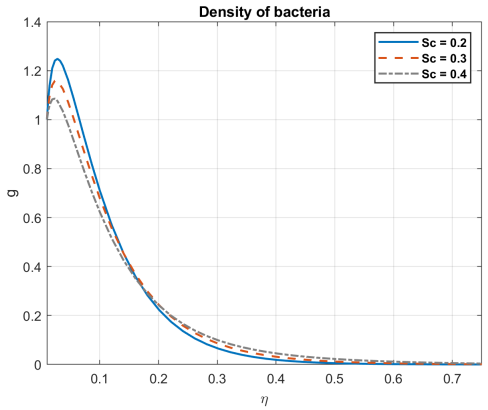

FIGURE 36. The influence of Sc on density of bacteria.

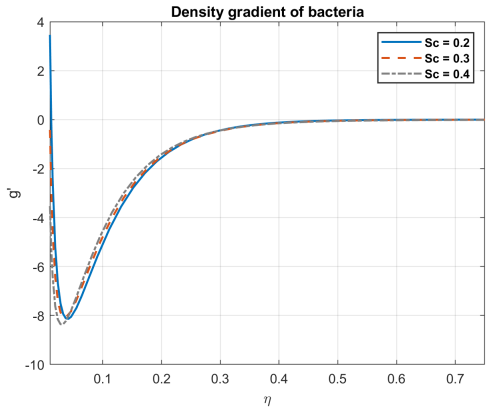

FIGURE 37. The influence of Sc on density gradient of bacteria.

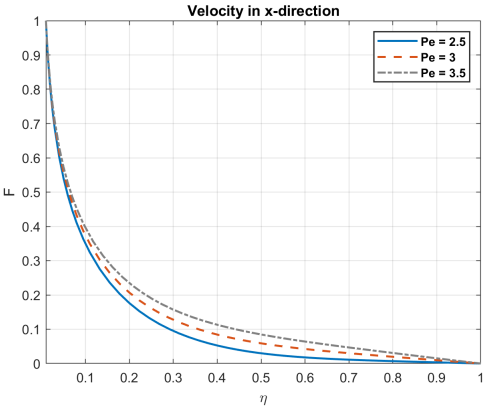

FIGURE 38.

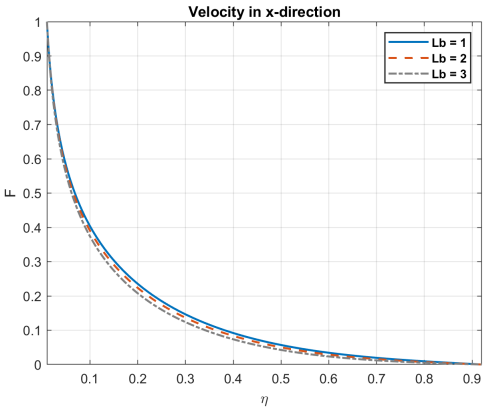

FIGURE 39. The influence of Lb on velocity in x-direction.

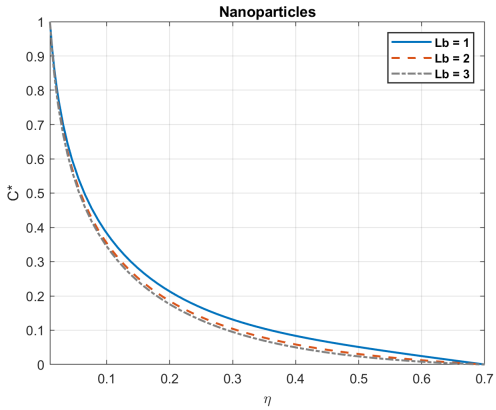

FIGURE 40. The influence of Lb on nanoparticles concentration.

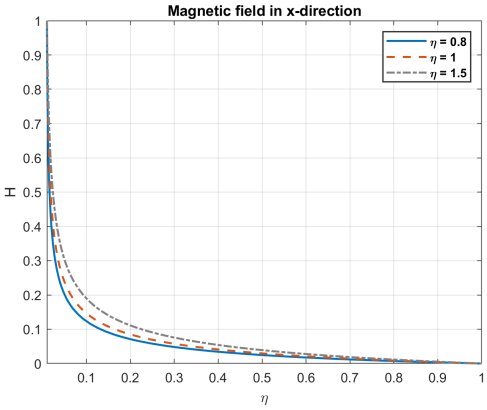

FIGURE 41. The influence of η_0 on magnetic field in x-direction.

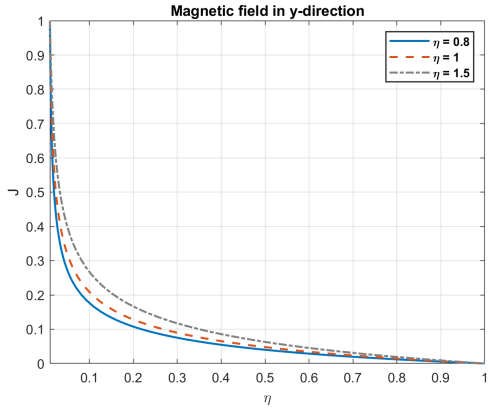

FIGURE 42. The influence of η_0 on magnetic field in y-direction.

Consequently, the fluid tends to transfer heat faster than the nanoparticles. This may result in a situation where the distribution of nanoparticles is less diversified than the fluid temperature. As a result, the fluid's velocity may be reduced for the nanoparticles. Figures 39 and 40 illustrate these observations.

4.12. **The significance of magnetic diffusivity η_0.**

Magnetic diffusivity (η_0) is a parameter that describes a material's ability to conduct magnetic fields. Magnetic diffusivity refers to the rate at which magnetic fields disperse or propagate inside a conducting material. Higher levels of magnetic diffusivity equate to quicker diffusion, implying that magnetic fields can spread across longer distances in less time. Figures 41 and 42 illustrate these observations.

5. CONCLUSION

In this work, a vertical thin needle used in medical surgery is employed to observe the flow of a nanofluid." The three different types of nanoparticles that make up the nanofluid are scattered in a base fluid, blood including $Fe_3O_4\, CuOandCu$. Gyrotactic bacteria are also present in the nanofluid. An understanding of this kind of flow property might be useful for minimally invasive surgery or medication distribution, two surgical techniques that depend on nanofluid flow. Besides, the incompressible liquid conducts current when there is a magnetic field existing.

This nanofluid model takes Thermophoresis and Brownian motion into account. The current study examined the impacts of many elements including Prandtl number, Pr, Brownian motion coefficient, D_B, Thermophoresis diffusion coefficient, D_T, microorganism diffusion coefficient, D_n, concentration difference, δc,temperature difference ratio, δt , Schmidt number, Sc, bioconvection Peclet number, Pe, Lewis number Lb, and magnetic diffusivity, η_0.

- An increase in Pr values cause a decrease in temperature, heat flow, nanoparticles, and bacterial density.
- As D_B values increase, there is a decrease in temperature, heat movement, and bacterial density, while velocity and nanoparticles rise.
- As D_T values grow, so do the temperature, heat flow, and bacterial density, while nanoparticle levels decrease.
- An analysis of the effects of the microbe diffusion coefficient reveals that both the velocity and the density of bacteria increase with D_n, levels.
- Upon analyzing the impact of concentration differences, we see that as δc values climb, velocity increases and temperature falls down.
- An analysis of the effects of temperature changes reveals that as δt values increase, so do temperature and velocity.
- When the Schmidt number, Sc, is examined, it is demonstrated that higher Sc values lead to higher bacterial densities and lower velocities.
- Analyzing bioconvection's impacts Peclet number shows that increasing Pe values lead to higher velocities.
- A study of the impact of Lewis number Lb indicates that decreasing velocity and nanoparticles are correlated with increasing Lb values.
- An analysis of the effect of magnetic diffusivity reveals that a rise in η_0 values correspond to an increase in the magnetic field.

TABLE 3. Nomenclature.

Latin Characters	
u, v	*Components of Velocity*
u_w, v_w	*Stretching velocity*
H_1, H_2	*Components of magnetic field*
x, r, t	*Independent variables*
H_{1w}, H_{2w}	*Stretching magnetic flux*
k^*	*Mean absorption coefficient*
g	*Acceleration due to gravity*
k_{hnf}	*Thermal conductivity of hybrid nanofluid*
D_B	*Brownian diffusion coefficient*
D_T	*Thermophoresis diffusion coefficient*
T	*Temperature of nanoparticles*
T_w	*Temperature at wall*
T_∞	*Ambient temperature*
c	*Concentration of nanoparticles*
c_w	*Concentration at wall*
c_∞	*Ambient concentration*
N	*Microorganisms' concentration*
N_w	*Microorganisms at wall*
N_∞	*Ambient microorganisms*
p_r	*Prandtl number*
$\mathcal{Q}_0$	*Volumetric rate of heat generation/absorption*
n	*Shape factor*
Sc	*Schmidt number*
Lb	*Lewis number*
w_c	*Cell swimming speed*
B_0	*Magnetic field strength*
b	*Thermal relaxation constant*
Pe	*Bioconvection Peclet number*
D_N	*Microorganism diffusion coefficient*
δt	*Temperature difference*
δc	*Concentration difference*
K^s, Q^s	*Differential coefficient functions*
S	*System variables*
G	*Group structure*
S_i	*Original dependent variables of the system*
$c_1, c_2, c_3, , , ,$	*Constants*
Greek Characters	
μ_e	*Magnetic Permeability*
ρ_{hnf}	*Density of hybrid nanofluid*
μ_{hnf}	*Viscosity of hybrid nanofluid*
α_{hnf}	*Thermal diffusivity of hybrid nanofluid*
η_0	*Magnetic diffusivity*
ρ_p	*Density of microorganisms*
ρ_f	*Density of base fluid*
σ^*	*Coefficient of mean absorption*
σ	*Electrical conductivity*
$(\rho c_p)_{hnf}$	*Volumetric heat capacity of hybrid nanofluid*
η	*Similarity variable*

References

[1] S. Ahmad, M. Ashraf, and K. Ali, *Bioconvection due to gyrotactic microbes in a nanofluid flow through a porous medium*, Heliyon, *6*(12) (2020), e05832.

[2] S. A. Alavi, A. Haghighi, A. Yari, and F. Soltanian, *A numerical method for solving fractional optimal control problems using the operational matrix of mott polynomials*, Computational Methods for Differential Equations, *10*(3) (2022), 755-773.

[3] K. A. M. Alharbi, U. Farooq, H. Waqas, M. Imran, S. Noreen, A. Akgül, D. Baleanu, S. M. El Din, and K. Abbas, *Numerical solution of maxwell-sutterby nanofluid flow inside a stretching sheet with thermal radiation, exponential heat source/sink, and bioconvection*, International Journal of Thermofluids, *18* (2023), 100339.

[4] A. Ali, S. Sarkar, S. Das, and R. N. Jana, *Investigation of cattaneo–christov double diffusions theory in bio-convective slip flow of radiated magneto-cross-nanomaterial over stretching cylinder/plate with activation energy*, International Journal of Applied and Computational Mathematics, *7*(5) (2021), 208.

[5] B. Ali, S. Hussain, Y. Nie, L. Ali, and S. U. Hassan, *Finite element simulation of bioconvection and cattaneo-christov effects on micropolar based nanofluid flow over a vertically stretching sheet*, Chinese Journal of Physics, *68* (2020), 654-670.

[6] R. Alluguvelli, C. S. Balla, K. Naikoti, and O. D. Makinde, *Nanofluid bioconvection in porous enclosure with viscous dissipation*, Indian Journal of Pure & Applied Physics, *60*(1) (2022), 78-89.

[7] A. M. Alwatban, S. U. Khan, H. Waqas, and I. Tlili, *Interaction of Wu's slip features in bioconvection of eyring powell nanoparticles with activation energy*, Processes, *7*(1) (2019), 859.

[8] N. A. Amirsom, M. Uddin, M. F. M. Basir, A. Ismail, O. A. Bég, and A. Kadir, *Three-dimensional bioconvection nanofluid flow from a bi-axial stretching sheet with anisotropic slip*, Sains Malays, *48*(5) (2019), 1137-1149.

[9] O. Anwar Bég, *Nonlinear multiphysical laminar nanofluid bioconvection flows: Models and computation*, Computational approaches in biomedical nano-engineering, (2018), 113-145.

[10] M. I. Asjad, N. Sarwar, B. Ali, S. Hussain, T. Sitthiwirattham, and J. Reunsumrit, *Impact of bioconvection and chemical reaction on mhd nanofluid flow due to exponential stretching sheet*, Symmetry, *13*(12) (2021), 2334.

[11] A. U. Awan, S. A. A. Shah, and B. Ali, *Bio-convection effects on williamson nanofluid flow with exponential heat source and motile microorganism over a stretching sheet*, Chinese Journal of Physics, *77* (2022), 2795-2810.

[12] C. S. Balla, C. Haritha, K. Naikoti, and A. Rashad, *Bioconvection in nanofluid-saturated porous square cavity containing oxytactic microorganisms*, International Journal of Numerical Methods for Heat & Fluid Flow, *29*(4) (2019), 1448-1465.

[13] N. Begum, S. Siddiqa, and M. Hossain,*Nanofluid bioconvection with variable thermophysical properties*, Journal of Molecular Liquids, *231* (2017), 325-332.

[14] N. Biswas, D. K. Mandal, N. K. Manna, and A. C. Benim, *Enhanced energy and mass transport dynamics in a thermo-magneto-bioconvective porous system containing oxytactic bacteria and nanoparticles: Cleaner energy application*, Energy, *263* (2023), 125775.

[15] A. Dawar, A. Saeed, S. Islam, Z. Shah, W. Kumam, and P. Kumam, *Electromagnetohydrodynamic bioconvective flow of binary fluid containing nanoparticles and gyrotactic microorganisms through a stratified stretching sheet*, Scientific Reports, *11*(1) (2021), 23159.

[16] S. Ghadikolaei, K. Hosseinzadeh, and D. Ganji, *Investigation on ethylene glycol-water mixture fluid suspend by hybrid nanoparticles $TiO_2 - CuO$ over rotating cone with considering nanoparticles shape factor*, Journal of Molecular Liquids, *272* (2018), 226-236.

[17] S. Ghadikolaei, K. Hosseinzadeh, and D. Ganji, *Investigation on three dimensional squeezing flow of mixture base fluid (ethylene glycol-water) suspended by hybrid nanoparticle $Fe_3O_4 - Ag$ dependent on shape factor*, Journal of Molecular Liquids, *262* (2018), 376-388.

[18] A. R. Haghighi and N. Aliashrafi,*A mathematical modeling of pulsatile blood flow through a stenosed artery under effect of a magnetic field*, Journal of Mathematical Modeling, *6*(2) (2018), 149-164.

[19] A. R. Haghighi and N. Aliashrafi, *Mathematical modeling of pulsatile blood flow and heat transfer under magnetic and vibrating environment*, International Journal of Heat and Technology, *36*(3) (2018), 783-790.

[20] A. R. Haghighi and R. Pralhad, *Mathematical modelling of blood flows under the effects of body forces and magnetism on human body*, International Journal of Biomedical Engineering and Technology, *2*(4) (2009), 295-302.
[21] A. R. Haghighi, N. Aliashrafi, and M. S. Asl, *An implicit approach to the micropolar fluid model of blood flow under the effect of body acceleration*, Mathematical Sciences, *14* (2020), 269-277.
[22] K. Hosseinzadeh, A. Asadi, A. Mogharrebi, M. Ermia Azari, and D. Ganji, *Investigation of mixture fluid suspended by hybrid nanoparticles over vertical cylinder by considering shape factor effect*, Journal of Thermal Analysis and Calorimetry, *143*(2) (2021), 1081-1095.
[23] K. Hosseinzadeh, S. Salehi, M. Mardani, F. Mahmoudi, M. Waqas, and D. Ganji, *Investigation of nano-bioconvective fluid motile microorganism and nanoparticle flow by considering mhd and thermal radiation*, Informatics in Medicine Unlocked, *21* (2020), 100462.
[24] K. Hosseinzadeh, S. Roghani, A. Mogharrebi, A. Asadi, and D. Ganji, *Optimization of hybrid nanoparticles with mixture fluid flow in an octagonal porous medium by effect of radiation and magnetic field*, Journal of Thermal Analysis and Calorimetry, *143* (2021), 1413-1424.
[25] P. P. Humane, V. S. Patil, M. Shamshuddin, G. R. Rajput, and A. B. Patil, *Role of bioconvection on the dynamics of chemically active casson nanofluid flowing via an inclined porous stretching sheet with convective conditions*, International Journal of Modelling and Simulation, *44*(4) (2024), 232-251.
[26] W. Khan and O. Makinde, *MHD nanofluid bioconvection due to gyrotactic microorganisms over a convectively heat stretching sheet*, International Journal of Thermal Sciences, *81* (2014), 118-124.
[27] W. A. Khan, A. Rashad, M. Abdou, and I. Tlili, *Natural bioconvection flow of a nanofluid containing gyrotactic microorganisms about a truncated cone*, European Journal of Mechanics-B/Fluids, *75* (2019), 133-142.
[28] A. Kuznetsov, *Nanofluid bioconvection: Interaction of microorganisms oxytactic upswimming, nanoparticle distribution, and heating/cooling from below*, Theoretical and Computational Fluid Dynamics, *26* (2012), 291-310.
[29] A. V. Kuznetsov, *Nanofluid bioconvection in porous media: Oxytactic microorganisms*, Journal of Porous Media, *15*(3) (2012), 233-248.
[30] A. V. Kuznetsov, *Nanofluid bioconvection in water-based suspensions containing nanoparticles and oxytactic microorganisms: Oscillatory instability*, Nanoscale research letters *6* (2011), 1-13.
[31] S. Mabrouk and A. Rashed, *Analysis of (3+ 1)-dimensional Boiti–Leon–Manna–Pempinelli equation via lax pair investigation and group transformation method*, Computers & Mathematics with Applications, *74*(10) (2017), 2546-2556.
[32] S. Mabrouk and M. Kassem, *Group similarity solutions of (2+ 1)- Boiti-Leon-Manna-Pempinelli lax pair*, Ain Shams Engineering Journal, *5*(1) (2014), 227-235.
[33] S. Mabrouk, M. Kassem, and M. Abd-el-Malek, *Group similarity solutions of the lax pair for a generalized Hirota–Satsuma equation*, Applied Mathematics and Computation, *219*(14) (2013), 7882-7890.
[34] A. Morgan, *The reduction by one of the number of independent variables in some systems of partial differential equations*, The Quarterly Journal of Mathematics, *3*(1) (1952), 250-259.
[35] W. N. Mutuku and O. D. Makinde, *Hydromagnetic bioconvection of nanofluid over a permeable vertical plate due to gyrotactic microorganisms*, Computers & Fluids, *95* (2014), 88-97.
[36] D. Pal and S. K. Mondal, *MHD nanofluid bioconvection over an exponentially stretching sheet in the presence of gyrotactic microorganisms and thermal radiation*, BioNanoScience, *8*(1) (2018), 272-287.
[37] P. Patil, B. Goudar, M. Patil, and E. Momoniat, *Bioconvective periodic mhd eyring-powell fluid flow around a rotating cone: Influence of multiple diffusions and oxytactic microorganisms*, Alexandria Engineering Journal, *81* (2023), 636-655.
[38] V. Puneeth, M. Sarpabhushana, M. S. Anwar, E. H. Aly, and B. J. Gireesha, *Impact of bioconvection on the free stream flow of a pseudoplastic nanofluid past a rotating cone*, Heat Transfer, *51*(5) (2022), 4544-4561.
[39] C. Raju and N. Sandeep, *Heat and mass transfer in mhd non-newtonian bio-convection flow over a rotating cone/plate with cross diffusion*, Journal of molecular liquids, *215* (2016), 115-126.
[40] C. S. Raju and N. Sandeep, *Dual solutions for unsteady heat and mass transfer in bio-convection flow towards a rotating cone/plate in a rotating fluid*, International Journal of Engineering Research in Africa,, *20* (2016),

161-176.

[41] M. V. S. Rao, K. Gangadhar, A. J. Chamkha, and P. Surekha, *Bioconvection in a convectional nanofluid flow containing gyrotactic microorganisms over an isothermal vertical cone embedded in a porous surface with chemical reactive species*, Arabian Journal for Science and Engineering, *46* (2021), 2493-2503.

[42] A. Rashad and H. A. Nabwey, *Gyrotactic mixed bioconvection flow of a nanofluid past a circular cylinder with convective boundary condition*, Journal of the Taiwan Institute of Chemical Engineers, *99* (2019), 9-17.

[43] A. Rashed and M. Kassem, *Group analysis for natural convection from a vertical plate*, Journal of computational and applied mathematics, *222*(2) (2008), 392-403.

[44] A. S. Rashed, E. H. Nasr, and M. M. Kassem, *Boundary layer analysis adjacent to moving heated plate inside electrically conducting fluid with heat source/sink*, International Journal of Heat and Technology, *38* (2020), 682-688.

[45] A. S. Rashed, E. H. Nasr, and M. M. Kassem, *Mathematical investigation for flow characteristics of laminar ferro-nanofluid incorporating cobalt ferrite nanoparticles*, Journal of Nano Research, *68* (2021), 52-69.

[46] A. S. Rashed, T. A. Mahmoud, and M. M. Kassem, *Behavior of nanofluid with variable brownian and thermal diffusion coefficients adjacent to a moving vertical plate*, Journal of Applied and Computational Mechanics, *7*(3) (2021), 1466-1479.

[47] A. S. Rashed, S. M. Mabrouk, and A. M. Wazwaz, *Unsteady three-dimensional laminar flow over a submerged plate in electrically conducting fluid with applied magnetic field*, Waves in Random and Complex Media, *33*(3) (2023), 505-524.

[48] A. S. Rashed, T. A. Mahmoud, and S. M. Mabrouk, *Enhanced flow and temperature profiles in ternary hybrid nanofluid with gyrotactic microorganisms: A study on magnetic field, brownian motion, and thermophoresis phenomena*, Journal of Applied and Computational Mechanics, *10*(3) (2024), 597-609.

[49] S. Saleem, H. Rafiq, A. Al-Qahtani, M. A. El-Aziz, M. Malik, and I. Animasaun, *Magneto jeffrey nanofluid bio-convection over a rotating vertical cone due to gyrotactic microorganism*, Mathematical Problems in Engineering, *2019*(1) (2019),3478037.

[50] R. Saleh, M. Kassem, and S. Mabrouk, *Exact solutions of Calgero–Bogoyavlenskii–Schiff equation using the singular manifold method after Lie reductions*, Mathematical Methods in the Applied Sciences, *40*(16) (2017), 5851-5862.

[51] S. A. A. Shah, N. A. Ahammad, E. M. T. E. Din, F. Gamaoun, A. U. Awan, and B. Ali, *Bio-convection effects on prandtl hybrid nanofluid flow with chemical reaction and motile microorganism over a stretching sheet*, Nanomaterials, *12*(13) (2022), 2174.

[52] B. Shen, L. Zheng, C. Zhang, and X. Zhang, *Bioconvection heat transfer of a nanofluid over a stretching sheet with velocity slip and temperature jump*, Thermal Science, *21*(6) (2017), 2347-2356.

[53] S. Siddiqa, N. Begum, S. Saleem, M. Hossain, and R. S. R. Gorla, *Numerical solutions of nanofluid bioconvection due to gyrotactic microorganisms along a vertical wavy cone*, International Journal of Heat and Mass Transfer, *101* (2016), 608-613.